The Astrophysical Journal, 790:48 (21pp), 2014 July 20 doi:10.1088/0004-637X/790/1/48
© 2014. The American Astronomical Society. All rights reserved. Printed in the U.S.A.

LUMINOUS AND VARIABLE STARS IN M31 AND M33. II. LUMINOUS BLUE VARIABLES, CANDIDATE LBVs, Fe II EMISSION LINE STARS, AND OTHER SUPERGIANTS*

Roberta M. Humphreys[1], Kerstin Weis[2], Kris Davidson[1], D. J. Bomans[2], and Birgitta Burggraf[2]
[1] Minnesota Institute for Astrophysics, 116 Church Street SE, University of Minnesota, Minneapolis, MN 55455, USA; roberta@umn.edu
[2] Astronomical Institute, Ruhr-Universitaet Bochum, Germany; kweis@astro.rub.de
Received 2014 April 21; accepted 2014 June 11; published 2014 July 2

ABSTRACT

An increasing number of non-terminal eruptions are being found in the numerous surveys for optical transients. Very little is known about these giant eruptions, their progenitors and their evolutionary state. A greatly improved census of the likely progenitor class, including the most luminous evolved stars, the luminous blue variables (LBVs), and the warm and cool hypergiants is now needed for a complete picture of the final pre-supernova stages of very massive stars. We have begun a survey of the evolved and unstable luminous star populations in several nearby resolved galaxies. In this second paper on M31 and M33, we review the spectral characteristics, spectral energy distributions, circumstellar ejecta, and evidence for mass loss for 82 luminous and variable stars. We show that many of these stars have warm circumstellar dust including several of the Fe II emission line stars, but conclude that the confirmed LBVs in M31 and M33 do not. The confirmed LBVs have relatively low wind speeds even in their hot, quiescent or visual minimum state compared to the B-type supergiants and Of/WN stars which they spectroscopically resemble. The nature of the Fe II emission line stars and their relation to the LBV state remains uncertain, but some have properties in common with the warm hypergiants and the sgB[e] stars. Several individual stars are discussed in detail. We identify three possible candidate LBVs and three additional post-red supergiant candidates. We suggest that M33-013406.63 (UIT301,B416) is not an LBV/S Dor variable, but is a very luminous late O-type supergiant and one of the most luminous stars or pair of stars in M33.

Key words: galaxies: individual (M31, M33) – stars: massive – supergiants

Online-only material: color figure, machine-readable table

1. INTRODUCTION—LUMINOUS BLUE VARIABLES, HYPERGIANTS, AND SUPERNOVA IMPOSTORS

An increasing number of objects initially classified as supernovae (SNe) in current surveys are not true SNe, i.e., the "SN impostors." Some of them appear to be pre-SN extreme events or giant eruptions like η Car. Others may be related to the classical luminous blue variables (LBVs) such as S Dor and AG Car (Humphreys & Davidson 1994), while those that are heavily obscured may be in a post-AGB or post red supergiant stage, i.e., the Intermediate Luminosity Red Transients (Bond 2011). There is considerable diversity in their observed properties; maximum luminosity and duration of the outburst. This diversity is the sign of a little explored field in stellar astrophysics. Very little is known about the progenitors of the giant eruptions and their evolutionary state.

Many of the SN impostors were initially classed as Type IIn SNe because of their narrow hydrogen emission lines which are usually ascribed to shock/circumstellar matter interactions. The coincidence of hydrogen envelopes, similar kinetic energies, and circumstellar material make the spectra of these objects and of Type IIn's look very similar. Only with subsequent observations that confirm that they are sub-luminous, or with photometry or spectroscopy showing that they do not develop as true SNe, are they recognized as impostors. See Van Dyk & Matheson (2012) for a recent review.

Many authors refer to these objects as LBVs, but most of the eruptions do not resemble the classical or normal LBV maximum light stage (Humphreys & Davidson 1994; Vink 2012). In quiescence an LBV or S Doradus variable is a moderately evolved hot star, with a B-type supergiant or Of-type/late-WN classification. An LBV eruption causes the wind to become dense and opaque, sometimes called a pseudo-photosphere at $T \sim 7000$–8000 K resembling the spectrum of an F-type supergiant. On an HR diagram the object thus appears to move toward the right. Since this alters the bolometric correction, the visual brightness increases by $\sim$2 mag while the total luminosity remains nearly constant (Wolf 1989; Humphreys & Davidson 1994, and numerous early references therein) or may decrease (Groh et al. 2009). Such an event can last for several years or even decades. Basic causes remain somewhat mysterious; most proposed explanations invoke an opacity-modified Eddington limit, subphotospheric gravity-mode instabilities, super-Eddington winds, and envelope inflation close to the Eddington limit (see Section 5 in Humphreys & Davidson 1994; Glatzel 2005; Owocki & Shaviv 2012; Vink 2012).

In rare cases, however, the luminosity substantially increases during outburst; these have been called giant eruption LBVs (Humphreys & Davidson 1994), η Car variables (Humphreys et al. 1999), or η Car analogs (Van Dyk 2005). The distinction between giant eruptions and the more common LBV or S Dor-type variability is often overlooked in the literature. They may be related and originate from similar types of stars, perhaps in the same evolutionary stage, but the physical cause may be different. Certainly the energetics of the eruptions and what we observe

* Based on observations with the Multiple Mirror Telescope, a joint facility of the Smithsonian Institution and the University of Arizona and on observations obtained with the Large Binocular Telescope (LBT), an international collaboration among institutions in the United States, Italy and Germany. LBT Corporation partners are: The University of Arizona on behalf of the Arizona university system; Istituto Nazionale di Astrofisica, Italy; LBT Beteiligungsgesellschaft, Germany, representing the Max-Planck Society, the Astrophysical Institute Potsdam, and Heidelberg University; The Ohio State University, and The Research Corporation, on behalf of The University of Notre Dame, University of Minnesota and University of Virginia.

are different. There are numerous questions about the origin of the giant eruptions, their relation to normal LBV outbursts, and perhaps even to SNe. These eruptions are important. They may account for considerable mass loss and they indicate that some instability has been overlooked in stellar theory.

Very little is known about the progenitors of these giant eruptions and their evolutionary state. They may have come from a range of initial masses and different evolutionary paths and the origin of the instability may be different. The observational record is sparse because these stars are rare and their importance has only been fully recognized in recent years. A greatly improved census of the likely progenitor class, including the most luminous evolved stars, the LBVs, and the warm and cool hypergiants is now needed for a complete picture of the final pre-SN stages of very massive stars. Few LBVs and hypergiants are known in our galaxy due to their rarity, uncertainties in distance, and the infrequency of the LBV eruptions. Even the Magellanic Clouds do not provide a large enough sample to properly determine the relative numbers, duration, and properties of these unstable and eruptive variables. For these reasons we have begun a census of the evolved and unstable luminous star populations in several nearby resolved galaxies.

In this first set of papers, we present the results of a spectroscopic survey of luminous and variable stars in the nearby spirals M31 and M33. In Paper I (Humphreys et al. 2013a), we discussed a small group of intermediate temperature supergiants, the warm hypergiants, and suggested that they were likely post-red supergiants. In this second paper, we review the spectral characteristics, spectral energy distributions (SEDs), circumstellar ejecta, and mass loss of the LBVs, candidate LBVs, emission line stars, and other luminous and variable stars in M31 and M33.

Our target selection and observations with the MMT/Hectospec and LBT/MODS1 are described in Paper I. We assign our targets to six different groups according to their spectroscopic and photometric characteristics described in Section 2. In Section 3 we present the evidence for circumstellar nebulae, dusty ejecta, and mass loss in many of these stars, and in the last section, we summarize our results.

2. CLASSIFICATION OF THE STARS

Since our targets include a variety of types, for discussion we have grouped them by their broad spectral characteristics and other known criteria such as previous variability as in the case of the LBVs. In this section we describe the characteristics of six groups. The LBVs/S Dor variables demonstrate a unique spectroscopic and photometric variability and are therefore discussed together as a separate group even though they share spectral characteristics with other groups. We discuss several individual stars and in many cases propose an alternative interpretation of their characteristics. See Paper I for a detailed discussion of the warm hypergiants. All of the stars for which we have spectra are listed in Table 1 in order of right ascension with their position, group type, spectral type where appropriate, and alternate names or designations. The M33C designation comes from an unpublished Hα survey by Kerstin Weis. In this paper, we use the galaxy name and the R.A. of the star as its designator for brevity and to save space in the tables. For completeness, the warm hypergiants from Paper I are included in Table 1, but are discussed only briefly in this paper. The visual photometry from Massey et al. (2006) was cross-identified with the near- and mid-infrared photometry from Two Micron All Sky Survey (2MASS; Cutri et al. 2003), the *Spitzer* surveys of M31 (Mould et al. 2008) and M33 (McQuinn et al. 2007; Thompson et al. 2009), and *Wide-Infrared Survey Explorer* (*WISE*; Wright et al. 2010). The first 10 entries are shown in Table 2 and the full table is available in the on-line edition. Table 2 also includes information on variability, when available, from Burggraf (2014) for the M33 stars and from Kaluzny et al. (1998) for M31 from the DIRECT survey. The Burggraf compilation includes data from several sources from ~1920 to the present, but most are since 1970. Eighteen of our stars in M33 are in common with Clark et al. (2012) and were observed at about the same time. The blue and red spectra in FITS format of all of the stars observed with the MMT/Hectospec are available at http:etacar.umn.edu/LuminousStars.

2.1. Luminous Blue Variables

Hubble and Sandage's classic 1953 paper on the brightest variables in M31 and M33 identified one object in M31 and four in M33 although Var A is now considered a post red supergiant, warm hypergiant (Humphreys et al. 1987, 2006, 2013a). There are now four confirmed LBVs in M31: AF And (Hubble & Sandage 1953; Luyten 1928; Sharov 1973; Humphreys 1975), AE And (Sandage & Tammann 1974; Luyten 1928; Sharov 1973; Humphreys 1975), Var 15 (Hubble 1929; Humphreys 1978), and Var A-1 (Rosino & Bianchini 1973; Sharov 1973; Humphreys 1978). The four in M33 are variables B, C, and 2 (Hubble & Sandage 1953; Sharov 1973; Humphreys 1975) and Var 83 (van den Bergh et al. 1975; Humphreys 1978). Here we discuss our recent spectra of the known LBVs and related objects.

AE And is one of the more interesting LBVs. It was the visually brightest star in M33 when it was discovered in "eruption" (Luyten 1928) and remained at visual maximum for twenty years. Its emission line spectrum closely resembles that of η Car. It has the anomalously strong 2507 Å Fe II line (Szeifert at al 1996) which has been attributed in η Car to a possible UV laser (Johansson & Letokhov 2004). In its current spectrum, several weak absorption lines are visible at wavelengths below 4100 Å; He I $\lambda\lambda$4026, 4009, 3819 Å, N II 3995 Å, and a weak Ca II K line (Figure 1). N II absorption at 5666 Å and 5670 Å is also present. These lines suggest a corresponding B2–B3 spectral type. The earlier 2003-2004 spectra show strong H and He I emission lines that have now weakened. Below 4100 Å these lines are now in absorption. These changes suggest that the wind has weakened.

Variable B in M33 had a high-mass-loss episode beginning in ~1982 (Szeifert et al. 1996; Massey et al. 1996), reaching an apparent visual brightness of ~14.9 mag at maximum. Its eruption lasted until at least 1998. The observational record is incomplete after that so it is not known when the episode ended, but it had definitely begun to decline by 2002 and it had returned to its hot quiescent or minimum state in our spectrum from 2003. Viotti et al. (2006) reported a visual magnitude of 17.5 for it in 2004 with a hot emission line spectrum. Comparison of our 2010 spectrum with the earlier spectrum from 2003 shows that the P Cygni absorption in the H and He I emission lines has weakened considerably and is now gone in the higher Balmer lines. Most of the Fe II and [Fe II] emission lines are also gone in 2010 (see Figure 2). The presence of numerous absorption lines of He I and Si III and N II 3995 Å suggests a B2 spectral type while the O II blend (4070–90 Å) and Si IV absorptions imply a slightly warmer B0–B1 spectral type for Var B.

Variable C in M33 has exhibited a series of maximum light episodes since its discovery; 1940–1953 (Hubble & Sandage

Table 1
Luminous Stars and Variables in M31 and M33: Spectroscopic Summary

Star Name	R.A. (2000)	Decl. (2000)	Spec. Group	Other Id/Notes/References
		M31		
	J004229.87[a]	+410551.8	Fe II Em. Line	[Fe II], He I, O I λ8446 em, see text
	J004242.33	+413922.7	Of/late-WN	P Cyg-type Massey et al. (2007)
	J004247.30	+414451.0	Intermed-Type	F2 Ia
AE And	J004302.52	+414912.4	LBV	see text, Figure 1
	J004313.02	+414144.9	...	weak-lined, foregrd
	J004318.57	+415311.1	...	G:V, foregrd
	J004320.97	+414039.6	Fe II Em. Line	O I λ7774 em, weak [Fe II]
	J004322.50	+413940.9	Warm Hypergiant	late A –F0 I (Paper I)
AF And	J004333.09	+411210.4	LBV	see text, Figure 5
	J004334.50	+410951.7	Of/late-WN	Ofpe/WN9 Massey et al. (2007), nebular em.
	J004337.16	+412151.0	Intermed-Type	F8 I
	J004341.84	+411112.0	Of/late-WN	P Cyg analog Massey (2006)
	J004350.50	+414611.4	Intermed-Type	A5 I, P Cyg H em. profiles
	J004406.32	+420131.3	Intermed-Type	F2 Ia
	J004411.36	+413257.2	Fe II Em. Line	weak Fe II em, He I, nebular em.
	J004415.00	+420156.2	Fe II Em. Line	[Ca II], [Fe II], wk He I em, double Hα profile, Figure 3
	J004417.10	+411928.0	Fe II Em. Line	Ca II, [Ca II], wk He I em., wk [Fe II], Figure 3
Var 15	J004419.43	+412247.0	LBV	see text
	J004424.21	+412116.0	Intermed-Type	F5 Ia, see text, Figure 6
	J004425.18[b]	+413452.2	Hot Supergiant	B0-1 Ia, P Cyg H em, broad wings, He I, O I 8446 em, see text
	J004442.28	+415823.1	Fe II Em. Line	O I λ7774 em, wk [Fe II], Hα asymmetric to blue, two emission features?
	J004444.52	+412804.0	Warm Hypergiant	F0 Ia (Paper I)
Var A-1	J004450.54	+413037.7	LBV	see text
	J004507.65	+413740.8	Intermed-Type	A5-A8 I, H em. P Cyg profiles, broad wings
	J004518.76	+413630.7	Intermed-Type	F2 I
	J004522.58	+415034.8	Warm Hypergiant	A2 Ia (Paper I)
	J004526.62	+415006.3	Intermed-Type	A2e I (Fe II em, P Cyg profiles) see text, Figure 7
	J004532.62	+413227.8	...	G:V, foregrd
	J004535.23	+413600.5	...	G:V, foregrd
		M33		
Var A	J013232.80	+303025.0	Warm Hypergiant	F8 Ia (Paper I), Humphreys et al. (1987, 2006)
M33C-4174	J013235.25	+303017.7	Fe II Em. Line	He I em. P Cyg, O I λ7774 em
	J013242.26	+302114.1	Fe II Em. Line	He I, [Fe II] em., Hα asymmetric to blue
UIT 008	J013245.41	+303858.3	Of/late-WN	O7-O8f I, see text, (Ofpe/WN9, WR5 Massey & Johnson (1998)), see text
M33C-14239	J013248.26	+303950.4	Fe II Em. Line	He I em.
UIT026	J013300.02	+303332.4	...	underexposed, em lines
M33C-4640	J013303.10	+303101.9	Intermed-Type	A0-A2e Ia, see text, very wk Fe II, wk He I em.
M33C-17194	J013307.51	+304258.4	...	composite sp., see text
N025981	J013308.95	+302956.2	Intermed-Type	A2 Ia, neb. em.,very wk He I em.
M33C-23048	J013309.12	+304954.5	Hot Supergiant	B0I + WN (Ofpe/WN9, UIT045, WR22 Massey et al. (1996))
M33C-13254	J013311.88	+303853.7	Intermed-Type	B8-A0 Ia + neb em., see text
M33C-4119	J013312.81	+303012.7	Hot Supergiant	B5 Ia, H, He I em., P Cyg
N033347	J013316.46	+303212.0	Intermed-Type	A5-A8 Ia, Hα P Cyg
	J013324.62	+302328.4	Fe II Em. Line	[Fe II] em., asymmetric Hα to blue, double em.
M33C-13560	J013327.26	+303909.3	Of/late-WN	Ofpe/WN9 UIT104, WR39, Massey et al. (1996)
N045901	J013327.40	+303029.4	Intermed-Type	F: pec I, see text, Figure 6
M33C-15742	J013332.64	+304127.2	Of/late-WN	WNL WR41 Massey & Johnson (1998)
M33C-7256	J013333.22	+303343.4	Fe II Em. Line	[Fe II], He I em., neb. em.
Var C	J013335.14	+303600.4	LBV	see text
N058746	J013335.29	+304146.0	foregrd	G: V + nebular em.
N061849	J013337.00	+303637.5	Intermed-Type	F5 -F8 Ia + neb. em.
M33C-19725	J013339.52	+304540.5	Hot Supergiant	B0.5: I pec[c], B517 Humphreys & Sandage (1980), see text
	J013340.6	+304137.1	Hot Supergiant	O8-O9 I + neb. em.
	J013341.28	+302237.2	Hot Supergiant	B2-3 Ia, H, He I em, P Cyg, 110-A Humphreys & Sandage (1980)
N073136	J013342.48	+303258.5	Hot Supergiant	B8 I + neb em
N075866	J013343.67	+303904.0	...	H II region
N078046	J013344.61	+303559.1	Hot Supergiant	B1-B2 Ia
M33C-18563	J013344.78	+304432.3	Hot Supergiant	OB + neb, H, He I em, UIT187 Massey et al. (1996)
Var B	J013349.23	+303809.1	LBV	see text, Figure 2
M33C-15731	J013350.12	+304126.6	Fe II Em. Line	Ca II, [Ca II], [Fe II], wk He I em., H P Cyg, UIT212 Massey et al. (1996), Figure 3
M33C-15235	J013351.45	+304057.0	Of/WN	He I P Cyg profiles, + neb. em.
N093351	J013352.42	+303909.6	Warm Hypergiant	F0 Ia (Paper I), M33C-13568
M33C-13206	J013353.58	+303851.8	Of/late-WN	Ofpe/WN9 UIT236, WR103 Massey & Johnson (1998), asymmetric H profiles
N097751	J013355.17	+303429.8	Hot Supergiant	early B-type + neb. em.

Table 1
(Continued)

Star Name	R.A. (2000)	Decl. (2000)	Spec. Group	Other Id/Notes/References
B324	J013355.96	+304530.6	Warm Hypergiant	A8-F0 Ia, UIT 247, (Paper I)
	J013357.73	+301714.2	Intermed-Type	A0 Ia, P Cyg profiles
M33C-9304	J013358.70	+303526.5	Hot Supergiant	B0-B1 Ia + WN, H P Cyg, asymmetric to red (B1Ia+WNE, UIT267 Massey et al. (1996))
N104139	J013358.92	+304139.4	Intermed-Type	F5 Ia, neb. em.
M33C-8094	J013359.89	+303427.3	Hot Supergiant	B0-B1 I + neb. em.
N107775	J013401.04	+303619.5	Hot Supergiant	mid-B-type, He II em. very broad + neb em
M33C-12568	J013401.91	+303819.3	Of/late-WN	H em profiles very asymmetric to red
	J013406.63	+304147.8	Hot Supergiant	O9.5 Ia, see text,B416 Humphreys & Sandage (1980), UIT301 Massey et al. (1996)
M33C-21386	J013406.78	+304727.0	Of/late-WN	WN7+neb, WR123, UIT 303 Massey et al. (1996)
Var 83	J013410.93	+303437.6	LBV	see text
N124864	J013415.19	+303704.0	Intermed-Type	early A-type + neb em
N125093	J013415.38	+302816.3	Warm Hypergiant	F0-F2 Ia, (Paper I)
M33C-7292	J013416.10	+303344.9	Hot Supergiant	B2.5 Ia, UIT341, B526, two stars, see text Humphreys & Sandage (1980)
	J013416.44	+303120.8	Hot Supergiant	B2-B3 Ia
Var 2	J013418.36	+303836.9	LBV	see text, Figure 5
	J013422.91	+304411.0	Hot Supergiant	B8 Ia, H P Cyg
	J013424.78	+303306.6	Hot Supergiant	B8-A0 Ia, Hα asymmetric to blue
	J013426.11	+303424.7	Fe II Em. Line	[Ca II], weak [Fe II], He I em, H lines asymmetric to red, Figure 3
	J013429.64	+303732.1	Hot Supergiant	B8 Ia, Hα P Cyg, broad wings
	J013432.76	+304717.2	Of/late-WN	Ofpe/WN9 Massey et al. (2007) + strong neb. em.
	J013442.14	+303216.0	Intermed-Type	A8 Ia, see text, Figure 6
	J013459.47	+303701.9	Fe II Em. Line	weak [Fe II], He I em.
	J013500.30	+304150.9	Fe II Em. Line	[Fe II]
GR 290	J013509.73	+304157.3	Of/late-WN	M33-V532, Romano's star, see text, Figure 5

Notes.

[a] Massey et al. (2007) labeled this star peculiar because of an absorption line spectrum characteristic of an F-type star together with Fe II and hydrogen emission lines. This star is only about 1 arcsec from a small cluster in M31 which was probably contaminating its spectrum in their survey. Our spectrum observed with the LBT/MODS1 was obtained under good seeing conditions and the cluster was kept off the slit. The star is an Fe II emission line star. He I λ4026 is present in absorption, and there are no F-type absorption lines.

[b] The spectrum may have changed since Massey et al. (2007). The blue spectrum shows absorption lines typical of early B-type supergiants while a strong O I λ7774 line common in A to F-type supergiants is present in the red.

[c] Several of the He I absorption lines appear to be double including λ4026, 4387, 4471, and 6678 due to emission in the line core. Hα and Hβ are asymmetric with a second emission component on the red side.

1953), 1964–1970 (Rosino & Bianchini 1973), and 1982–1993 (Humphreys et al. 1988; Szeifert et al. 1996). The latter eruption was probably in decline by 1993 as evidenced by its visual photometry and apparent temperature of ~15,000 K, indicating that it was in an extended transition to its hotter state at that time (Szeifert et al. 1996). It had returned to its quiescent state by late 1998 (see Burggraf et al. 2014), but quickly entered a short maximum light stage beginning in 2001 and lasting until 2005 based on the spectra and photometry published by Viotti et al. (2006) and Clark et al. (2012). This short maximum may be similar to the brief brightening reported by Rosino & Bianchini (1973). Our spectrum from 2010 confirms that Var C had returned to its hot quiescent stage. The presence of absorption lines of N II 3995 Å several He I absorption lines, and S IV 4089 Å suggest a corresponding B1–B2 spectral type. Another LBV eruption began in 2011 (Humphreys et al. 2013b). Its pre-eruption spectrum and a recent spectrum after the onset of the current maximum are described in Humphreys et al. (2014).

Var C has been highly unstable since its eruption in the 1980s with a shorter outburst in 2001–2005, and the current brightening beginning in 2011. We suggest that Var C needs either a longer duration normal LBV eruption like the episode in the 1940s or perhaps a giant eruption to stabilize it in an extended quiescent stage.

Var 83 in M33 has strong emission lines of hydrogen, He I and Fe II plus absorption lines of N II and He I and the Ca II K line in absorption. The presence of the He I absorption lines of λ4026, 4009, 4144 Å, and N II λ3995 Å suggests a corresponding B2 to B3 spectral type. The Balmer lines also show asymmetric profiles with very broad wings.

Var A-1 in M31 also shows N II lines in absorption and in addition to hydrogen and He I emission several Fe II and [Fe II] lines are present. Var A-1's earlier spectrum from 2003 showed absorption lines of He I similar to Var 83. In the current spectrum these are weaker and the Balmer emission lines and P Cygni profiles are much stronger.

AF And and *Var 15* in M31 in quiescence have spectra like the Of/late WN stars with strong N III emission lines and strong He I and hydrogen emission with P Cygni profiles. AF And's current spectrum shows little change from 2003–2004. Like AF And and Var 15, *Var 2* in M33 has nitrogen emission lines plus He II λ4686 in emission. The spectra of AF And and Var 2 are shown in Figure 5 with other Of/late WN stars.

Romano's star, also known as GR 290 and M33-V532, (Romano 1978) is often considered an LBV or candidate LBV (Polcaro et al. 2003, 2011; Sholukhova et al. 2011). It does indeed exhibit photometric variability, as much as 1.5 mag in the blue, but it is not known to show the spectroscopic transition from a hot star (visual minimum) to the optically thick cool wind resembling an A- to F-type supergiant at visual maximum that is characteristic of the LBV/S Dor phenomenon. Instead its spectra exhibit variability from WN8 at minimum to WN11 at visual maximum (Sholukhova et al. 2011; Polcaro et al. 2011) with a corresponding apparent temperature range from about

Table 2
Multi-wavelength Photometry

Star	*U*	*B*	*V*	*R*	*I*	*J*	*H*	*K*	3.6 μm[a]	4.5 μm[a]	5.8 μm[a]	8 μm[a]	3.4 μm[b]	4.6 μm[b]	12 μm[b]	22 μm[b]	Var
								M31									
M31-004229.87	18.5	19.1	18.8	18	18.2	...	...	...	12.4	11.6	11	10.2	12.6	11.7	9.5	7.2	
M31-004242.33	17.85	18.7	18.6	18.2	18.1	...	...	...	...	...	...	...	...	...	...	...	
M31-004247.30	17.1	16.9	16.4	16	15.6	15.3	15	15	...	...	...	...	14.55	14.44	11.78	8.66	
AE And	16.35	17.25	17.4	17.2	17.2	16.39	15.89	15.8	15.84	15.43	14.93	12.84	15.4	15.1	11.1	7	LBV
M31-004320.97	19	19.8	19.2	18.4	17.9	17.1	16.7	15.2	13.3	12.7	11.8	10.9	13.5	12.5	9.2	7.2	
M31-004322.50	20.7	21.2	20.3	19.9	19.2	...	...	...	14.9	14.6	14.4	13.5	15.7	15.5	12.3	9.1	
AF And	16.4	17.3	17.3	17.5	17.4	15.8	15.37	15.41	...	...	...	...	14.8	15	11.3	8	LBV
M31-004334.50	17.3	18.2	18.1	17.8	17.7	16.5	15.6	14.7	...	...	...	...	...	...	...	...	
M31-004337.16	19.6	18.9	17	16.55	16.15	16.5	15.6	14.7	...	...	...	...	14.95	14.11	11.06	9.27	
M31-004341.84	17.2	17.95	17.5	17.1	16.8	16.4	16.2	15.6	15.6	14.8	14.2	13.1	...	...	...	...	

Notes.
[a] *Spitzer*/IRAC.
[b] *WISE*.

(This table is available in its entirety in a machine-readable form in the online journal. A portion is shown here for guidance regarding its form and content.)

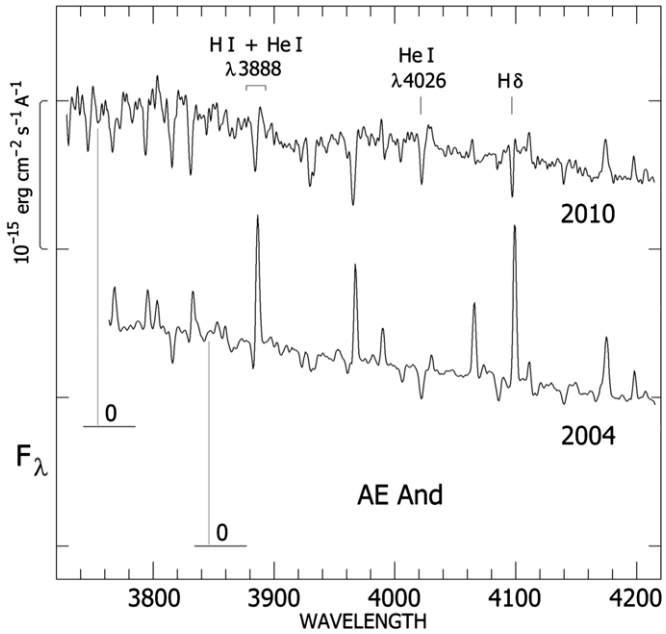

Figure 1. Spectra of AE And from 2010 and 2004. Although they are shown flux calibrated for comparison, the flux calibrator was observed at a different time than the 2010 spectrum. Therefore, it should not be used for any absolute measurements. F_λ is plotted with the scale for both spectra, but for clarity the zero points are offset as indicated.

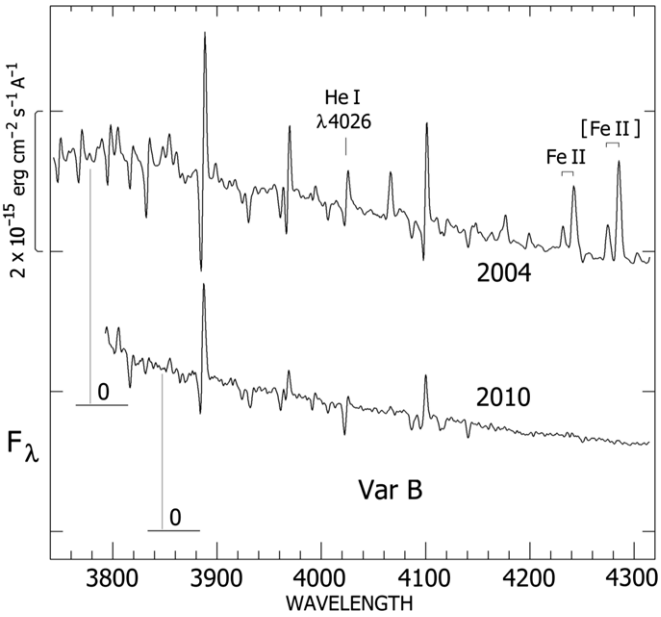

Figure 2. Spectrum M33 VarB in 2010 and 2004. They are shown flux calibrated for comparison although the flux calibrator was observed at a different time than the 2010 spectrum and should not be used for any absolute measurements. As in Figure 1, F_λ is plotted with the scale for both spectra, but for clarity the zero points are offset as indicated.

42,000 K to 22,000 K (Sholukhova et al. 2011). Our current spectrum from 2010 October shows He II λ4686 plus the N III emission lines characteristic of the late WN stars in addition to prominent emission lines of H and He I and is consistent with a spectrum intermediate between its two states. See Clark et al. (2012). Our spectrum is shown in Figure 5.

Since many LBVs in quiescence have the spectral characteristics of late-type WNs, it is interesting to speculate on whether Romano's star is a hot star in transition to the LBV stage or if it may be in a post-LBV state (Polcaro et al. 2011).

2.2. Fe II Emission-line Stars

The distinguishing characteristic of this group is a blue continuum with strong hydrogen emission, Fe II emission, and a lack of absorption lines which would otherwise permit a spectroscopic classification. It must be remembered though that the presence of Fe II emission is ubiquitous in astronomical spectra. Fe II has low excitation energies and is observed in many different types of stars with a wide range of luminosities and temperatures. Furthermore, the spectra of the stars in this group are not all alike. Some of them have strong He I emission, and some have [Fe II] emission while others do not. Those with He I emission are presumably hot supergiants with surface temperatures at or above 20,000 K. [Fe II] and [O I] emission is a common characteristic of the B[e] and sgB[e] stars. Since not all of these stars have these emission lines, but their spectra all show Fe II emission, in this paper, we call them Fe II emission line stars. Clark et al. (2012) called them "iron stars." The notes in Table 1 indicate if [Fe II], He I, or other lines of interest are present.

Many of these stars also have significant infrared excess emission over and above what we would expect from free–free emission from their stellar winds. Five of the six M31 stars in this group and six of the nine in M33 have an infrared excess due to circumstellar dust. In a few cases an IR excess longward of 8 μm is present probably due to contaminating emission from surrounding H II nebulosity. The SEDs for these stars are discussed in the next section. Some of these same stars also have emission lines of [N II] 6548 Å and 6583 Å and [S II] 6717 Å and 6731 Å. Given the lack of or weak [O III] and [O II] emission in their spectra, the signature emission lines of an H II region, the red [N II], and [S II] emission lines may be formed in their circumstellar ejecta and can be used to estimate the gas density. This special subclass of our stars are discussed in a separate paper by K. Weis et al. (2014, in preparation).

Four of these stars are of particular interest because, like the warm hypergiants described in Paper I, they have the [Ca II] doublet in emission. Their spectra are dominated by strong hydrogen emission with broad wings at Hα and Hβ and some have P Cygni profiles. They all show relatively weak Fe II emission and no or very weak He I emission lines. The MODS1 red spectra of M33C-15731 and M31-004417.10 confirm that the Ca II triplet is likewise in emission and they also have the O I triplets at λ7774 Å and O I 8446 Å in emission. The latter is much stronger than the λ7774 Å feature likely due to λ8446 fluorescence with Lyman β. The only apparent absorption lines in these two stars are He I 4026 Å and 4009 Å and a weak K-line. In addition to the [Ca II] emission, the spectra of M33-013426.11 and M31-004415.00 show weak He I emission and no obvious absorption lines. M31-004415.00 also has a double or split Hα emission profile like some of the warm hypergiants. Its O I 7774 Å line is also in emission. All four stars also have an infrared excess due to dust. The blue and red spectra of these four stars are shown in Figure 3.

One of the Fe II emission line stars, M31-004229.87, was described as peculiar by Massey et al. (2007) because of an absorption line spectrum characteristic of an F-type star with strong Ca II H and K lines together with Fe II and hydrogen emission lines. We were suspicious that it might be a warm hypergiant (Paper I) and consequently obtained a long slit spectrum of it with LBT/MODS1 which instead shows that

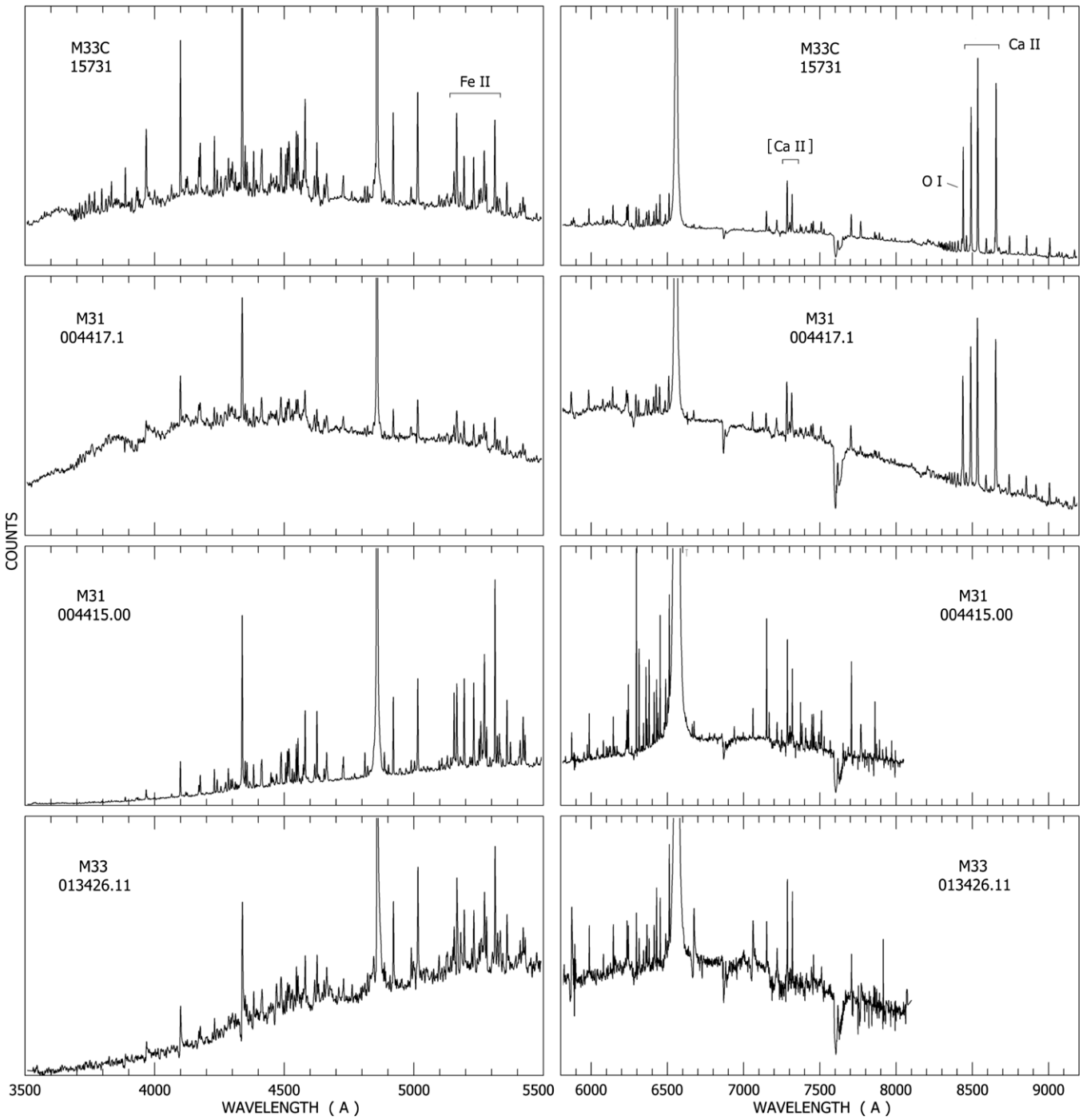

Figure 3. Spectra of the four Fe II emission line stars with [Ca II]. The two upper spectra were observed with the LBT and show the Ca II triplet.

M31-004229.87 is indeed an Fe II emission line star. He I λ4026 is present in absorption, and there are no F-type absorption lines and also no Ca II or [Ca II] emission. We noticed that there is a small cluster only about 1″ to the south of the star which is the likely source of the strong H and K lines in the Hectospec spectrum in their Figure 13 (Massey et al. 2007).

Clark et al. (2012) included M33-013406.63, also known as B416 (Humphreys & Sandage 1980) and UIT 301 (Massey et al. 1996), in his group of "iron stars." It does indeed have weak Fe II and [Fe II] emission, but its spectrum also shows Si IV absorption at λ4089 and λ4116, N III at λ4097, and weak He II λ4200 absorption plus He I emission lines (Figure 4). Based on its absorption lines, we classify it as a hot supergiant (Section 2.4) with spectral type O9.5 Ia. As we show in Section 3.1 and discuss in Section 4, M33-013406.63 is a very luminous and potentially very interesting star, although we do not consider it an LBV or LBV candidate.

Massey et al. (2007) called several of these stars "hot LBV candidates," that is, stars in the hot quiescent or minimum light stage of LBV/S Dor variables. However, LBVs in quiescence typically show several absorption lines found in the spectra of normal hot supergiants, such as AE And, Var B, and Var C, or spectral characteristics in common with the Of/WN stars or late WN's, like Var 2 and AF And. Except for the hot supergiant M33-013406.63, the Fe II emission line stars do not share this characteristic. Given the presence of an infrared

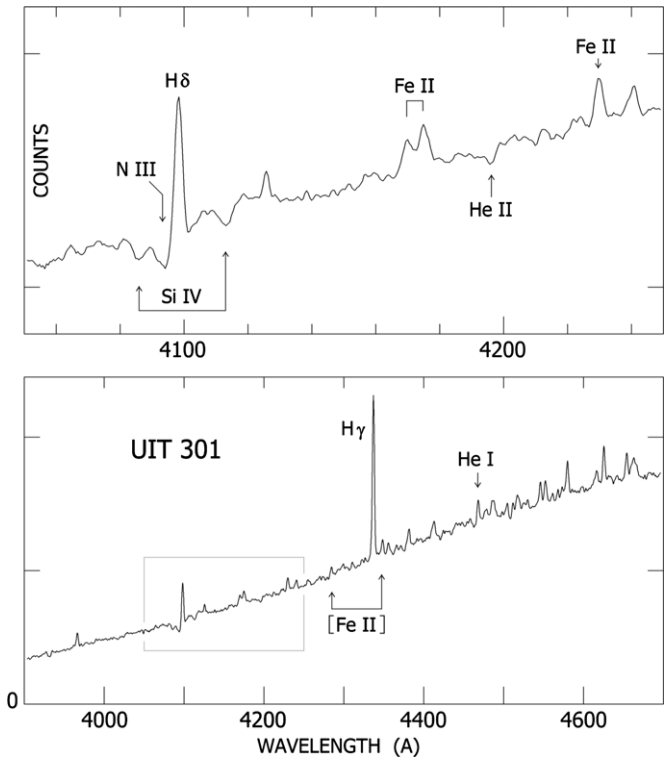

Figure 4. Blue spectrum of M33-013406.63 (B416,UIT301). The upper panel show the region around Hδ with the Si IV, N II, and the He II absorption lines identified.

excess plus spectroscopic evidence of circumstellar ejecta in many of these stars, they may indeed be candidate LBVs, in a post-LBV or post-giant eruption state, or even post-RSGs since some of these stars share some characteristics with the warm hypergiants. Their SEDs, mass loss, and luminosities are presented in Section 3 and their possible relation to the LBV phase and post-red supergiants is discussed in the last section.

2.3. Of/late-WN Stars

These stars have the well-known spectral characteristics of the Of and late-WN type stars with emission lines of N III and He II λ4686 in addition to strong hydrogen and He I emission. The blue spectra of two late-WN stars, M33C-15235 and M31-004242.33 are shown in Figure 5 together with Romano's star (V532), and the LBVs AF And and Var 15 which share these spectral characteristics in quiescence.

2.4. Hot Supergiants with Absorption and Emission Lines

This group includes the luminous O and B-type stars, some with hydrogen and other emission lines, with an absorption line spectrum that allows the assignment of an approximate spectral type. Here we describe a few hot supergiants with interesting spectral characteristics, such as Fe II emission and possible spectral variability.

The late-O type spectrum of M33-013406.63 with weak Fe II emission was described in the previous section. M33C-7292, also known as B526 (Humphreys & Sandage 1980) and UIT 341 (Massey et al. 1996), is another example of a star with the absorption line spectrum of a hot supergiant with hydrogen emission plus weak Fe II emission lines. Its spectrum was discussed previously by Monteverde et al. (1996), who classified it B2.5 Ia, but did not note the presence of the weak Fe II emission lines. Clark et al. (2012) called it a candidate LBV and their brief

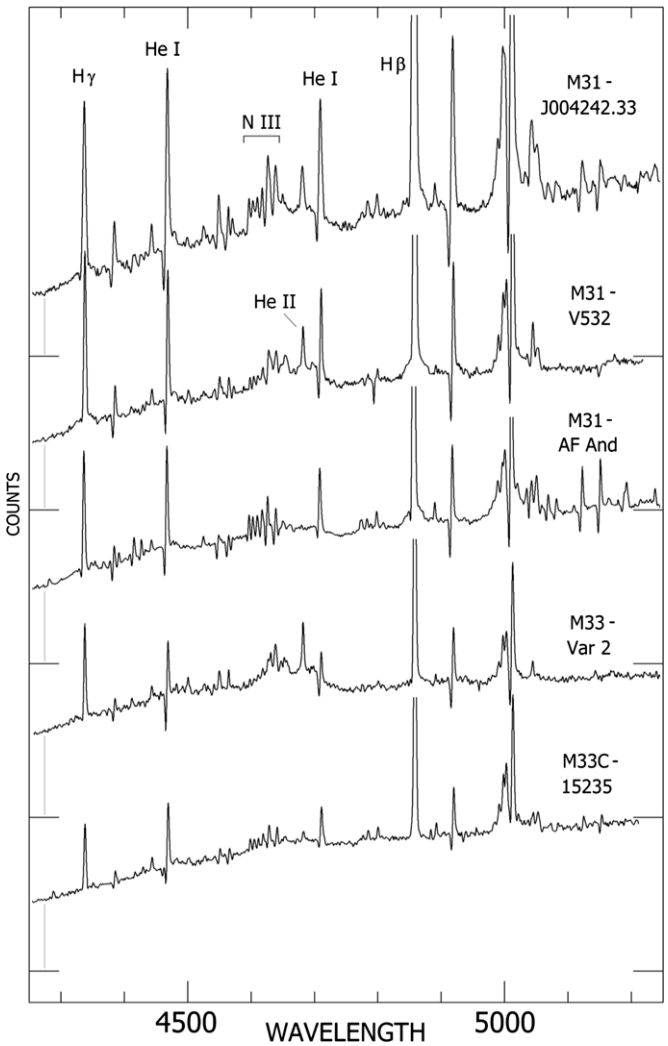

Figure 5. Spectra of five Of/late-WN stars: the LBV/S Dor variables AF And and M33 Var2, V532 (Romano's star) in 2010, and two late-WN stars, M33C-15235 and M31-004242.33.

description resembles our spectrum. However, Monteverde et al. (1996) noted that M33C-7292/B526 might be two stars based on their acquisition image. *Hubble Space Telescope* (*HST*)/Wide-Field Planetary Camera 2 (WFPC2) images indeed show that it is two stars of about equal brightness separated by less than 1″. Massey's (2006) images are slightly longated; the northernmost component is much brighter in Hα and is therefore the likely source of the emission lines, but the other component is brighter in the *U* band. The published spectra are all likely composite. We include it in Table 1 but do not discuss it further until spectra of the separate components can be obtained.

M31-004425.18 has the absorption line spectrum of an early B-type supergiant, but the spectrum appears to have changed from the one shown by Massey et al. (2007), who called it a cool LBV candidate. Our spectrum shows absorption lines of He I at λ4026, 4009, 4144, 4387, and 4471, but He I λ5015, 5876, and 6678 are in emission. In addition, O II λ4346-4351, Si III λ4553, and O II/C III λ4647–51 are present in absorption as are the N II lines from λ5666–5730 Å. On the basis of these absorption lines, we classify the star B2-B3 I. The hydrogen lines are in emission with strong P Cygni absorption and Hβ and Hα have very broad wings. The Mg II λ4481 line in Massey's et al.'s spectrum (their Figure 19) is much weaker in our spectrum. These

spectroscopic changes suggest a shift to warmer temperatures from 2006 when Massey's et al.'s spectrum was obtained to 2010. M31-004425.18 may be an LBV candidate, although there are no obvious Fe II emission lines in either spectrum. In the DIRECT survey, the star exhibits limited variability of $\approx \pm 0.1$ mag. *HST* images show a single star. This star is discussed further in Section 4.2 as a less luminous LBV/S Dor candidate.

Clark et al. (2012) have discussed the evidence for long-term small spectroscopic variations in M33C-19725 (M33-013339.52, B517; Humphreys & Sandage 1980). The star also shows evidence of photometric variability on the order of ± 0.3 mag (Burggraf 2014). We classify it B0.5:I based on the He I, Si IV λ4089, and 4116 plus Si III λ4553 absorption lines. However, we also note some peculiarities. For example, the He I absorption lines at λ4026, 4471 and 5876 Å appear to be double due to emission in the core. This structure is also present in Hγ and Hδ, although both Hβ and Hα have asymmetric profiles with P Cygni absorption plus a second emission component on the red side. The star is embedded in a small H II region which may provide a variable contribution to the emission lines depending on the aperture size, although the nebular lines are weak.

Our spectrum of M33C-13254 shows strong nebular emission superimposed on the absorption line spectrum of a late B- to early A-type supergiant. However, this differs significantly from its spectrum from 2007 October (Burggraf 2014) which shows the N III triplet Wolf–Rayet feature and He II λ4686 Å in emission. Earlier, Conti & Massey (1981) had classified it WNL. M33C-13254 is in the H II region NGC 592, a crowded field, so it is possible the 1.″5 fiber included more than one star, but there is no evidence of WR features in our spectrum. Its photometric record summarized by Burggraf (2014) shows an increase by one magnitude in B and V between 2002 and 2007, and in 2011 its $B-V$ color varied from 0.2 to 0.4 mag. However, a one magnitude increase is not sufficient to explain a transition from a WR star to a late B-type supergiant due to an LBV-like dense wind event. The expected shift in the apparent temperature would require a change in the bolometric correction of ≈2.5 mag. Furthermore, there are no P Cygni profiles in the B supergiant spectrum which would be expected from a wind. Therefore, despite the close agreement between the fiber position with the star's position in the Massey et al. (2006) catalog,[3] we suspect that this is a misidentification.

These and several other stars classified as hot supergiants are listed in Table 1 with their spectral types.

2.5. Intermediate-type Supergiants (A- to G-type)

The intermediate-type or "yellow" supergiants include the visually most luminous stars in their respective galaxies. Many of the most luminous A- and F-type supergiants often exhibit hydrogen in emission due to mass loss and winds, a characteristic shared by the stars in this group. A few of these stars of special interest are described here.

Unlike the warm hypergiants in Paper I, only one of these intermediate type supergiants, M33-013442.14, has an infrared excess due to dust Section 3. Our spectrum also reveals what may be a significant change from the one published by Massey et al. (2007), who called it a questionable hot LBV candidate. Instead, it has the absorption line spectrum of a late A-type supergiant with Hα and Hβ in emission with P Cygni profiles. The O I λ7774 Å triplet, a well-known luminosity indicator in evolved stars from spectral types A to early G-type supergiants (see Arellano Ferro et al. 2003 and references therein) is present in absorption. It does not show any Fe II or [Ca II] emission. It is unclear if this apparent spectral change is real, though, because Massey et al.'s published spectrum (their Figure 17) has low resolution and low signal-to-noise ratio (S/N) in the continuum and shows only Hα and Hβ in emission plus what look like Fe II absorption lines. We conclude that there is no evidence for a real spectroscopic change. Our blue and red spectra are shown in Figure 6.

The spectrum of M31-004526.62, with Fe II emission lines and prominent P Cygni profiles in the multiplet 42 Fe II lines, closely resembles that of M31-004444.52, one of the warm hypergiants described in Paper I. M31-004526.62 has strong hydrogen emission lines with broad wings and P Cygni profiles, [N II] emission, and the absorption line spectrum of an early A-type supergiant. K. Weis et al. (2014, in preparation) conclude that it has a high density circumstellar nebula, although it does not have the [Ca II] emission or an infrared excess due to dust. Its blue and red spectra are shown with M31-004444.52 in Figure 7.

M33C-4640 is another star with an early A-type absorption spectrum plus weak Fe II emission lines at λ5018 and from 5100 to 5400 Å, but without the deep P Cygni features seen in M31-004526.62. He I is also in emission.

Because of our interest in the warm hypergiants, which show evidence for circumstellar ejecta and high mass loss events, we also observed several of the more luminous F-type supergiant candidates in M31 from Drout et al. (2009). We noticed that the O I λ7774 Å triplet, the strong luminosity indicator, is not present in about half of the stars we observed, a fact that was also noted by Drout et al. (2009). We find that some of these stars are probable foreground stars. With their high velocities, they are likely Population II or Thick Disk stars in the Galactic Halo. Their spectral types are included in Table 1.

One of their F-type supergiants, M31-004424.21, with very strong O I λ7774 absorption, also has strong Hα emission and nebular [N II] λλ6548, 6584 and [S II] λλ6717, 6731 emission, but no [O III] or [O II] emission. The [N II] and [S II] emission may originate in a circumstellar envelope (see K. Weis et al. 2014, in preparation). As mentioned above, the [N II] and [S II] emission lines are present in several of our stars and are possible indicators of circumstellar ejecta discussed in the next section. Its blue and red spectra are shown with M33-013442.14 in Figure 6.

The paper by Drout et al. (2012) on the yellow and red supergiants in M33 was not available when we obtained our spectra. Some of the M33 stars in our intermediate type group are in their list of candidate supergiants. One of their "red supergiants," M33-013242.26, however, is actually an Fe II emission line star.

We conclude this section by mentioning N045901 in M33. Valeev et al. (2010) suggested that N045901 is an LBV candidate. However, contrary to their description based on a low S/N spectrum, our spectra show an F-type absorption line spectrum with Hα and weak Hβ emission. The luminosity sensitive O I 7774 triplet is very weak. There are no Ca II, [Ca II], or Fe II emission lines except for two [Fe II] lines at λ5158 Å and 7155 Å. Its reported small light variations of the order of ± 0.2 mag are typical of these kinds of stars often referred to as α Cygni variability (see van Genderen & Sterken 2002, and references therein). Drout et al. (2012) classify it as a supergiant, but they do not report an equivalent width for the O I line,

[3] Hectospec fiber 01:33:11.85, +30:38:53.69, and 01:33:11.88, +30:38:53.7(Massey).

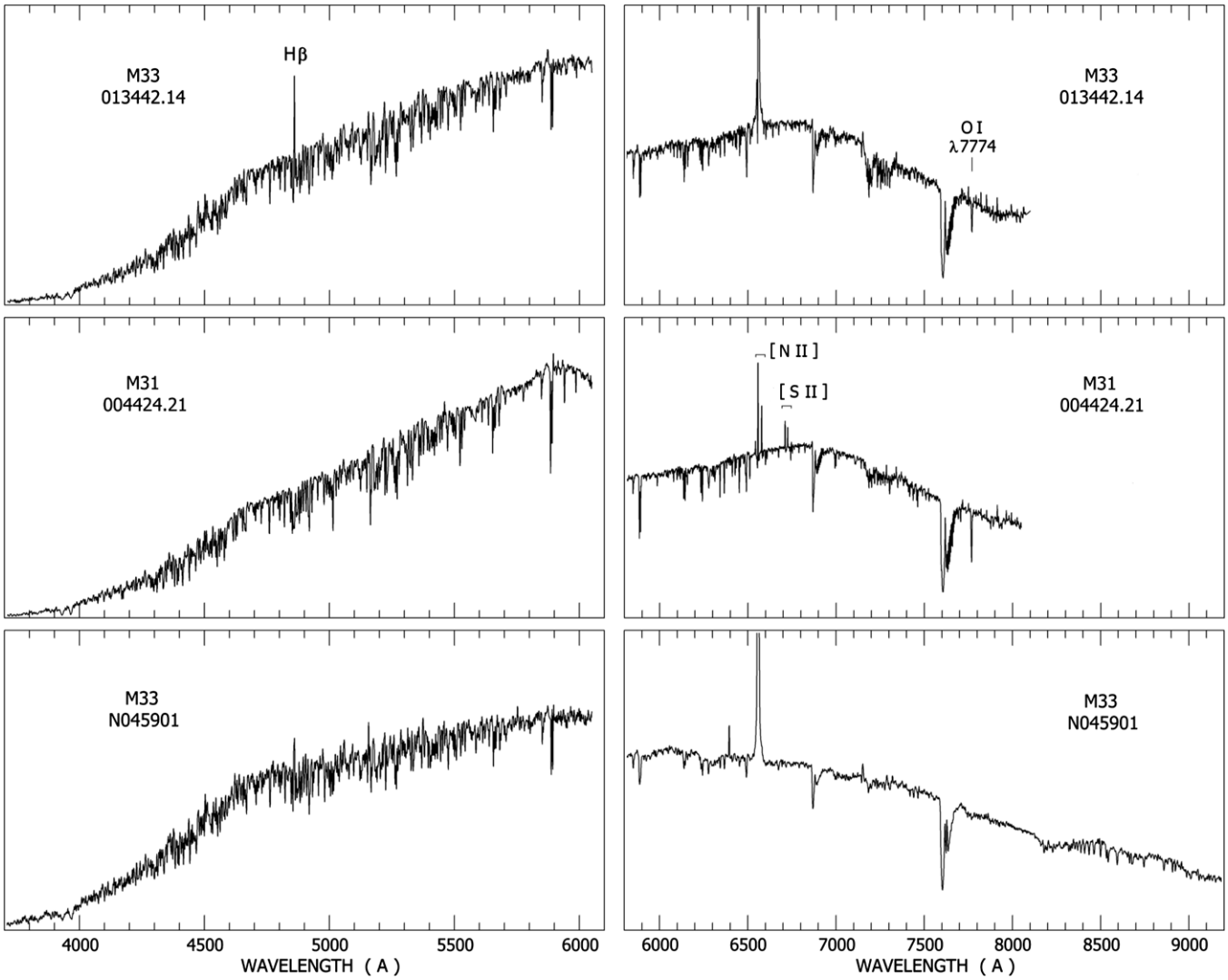

Figure 6. Spectra of the F-type supergiants discussed in Section 2.5.

one of their primary criteria for the F-type supergiants. This is consistent with the very weak O I feature in our spectra. N045901's one peculiar feature is a split or double Hα profile similar to those observed in some of the warm hypergiants. Evidence for doubling can also be seen in the weak Hβ emission line. Too little information is available about this star to be conclusive, but we doubt that it is an LBV candidate. Its blue and red spectra are shown in Figure 6.

2.6. The Warm Hypergiants

The warm hypergiants discussed in Paper I have A–F-type supergiant absorption line spectra and strong hydrogen emission. Several of these stars also show strong Fe II emission lines and weak [Fe II]. Their spectra are distinguished by the Ca II triplet and [Ca II] doublet in emission. They all have significant near- and mid-infrared excess radiation due to free–free emission and thermal emission from dust. In Paper I we suggest that these evolved stars are candidates for post-red supergiant evolution. Kraus et al. (2014) described one of them, M31-004522.57, as a sgB[e] star. It does have weak [Fe II] emission, but with absorption lines characteristic of an early A-type supergiant, not the B-type or veiled O-type spectrum expected for the sgB[e] stars.

Before concluding this section, we should mention that M33C-17194 is not included in any of the six groups discussed here. Our spectrum of it is composite with hydrogen emission, absorption lines of He I like a mid to late B-type supergiant, but also with absorption lines like a cooler star, and molecular band heads due to TiO beyond 5100 Å. Massey et al. (2007) classified as a WN star. We checked the *HST* images and find two stars only about 0.″4 apart in declination. The eastern component is blue and the probable WN star. The other star is red.

3. CIRCUMSTELLAR NEBULAE, DUSTY EJECTA, AND MASS LOSS

Most of the stars included in our spectroscopic program for M31 and M33 were selected specifically because they were known or candidate LBVs, emission line objects and known variables. So it is not surprising that many of them show spectroscopic evidence for the presence of circumstellar ejecta ranging from nebular emission lines to dust revealed by their long wavelength SEDs.

In Table 3 we list all of the stars that show one or more of the following indicators for circumstellar material; [N II] emission lines, Ca II and [Ca II] emission lines, and infrared

Table 3
Stars with Circumstellar Nebulae and Dust

Star Name	Spec. Group	[N II]	Ca II/[Ca II]	IR Excess	Comments
		M31			
M31-004229.87	Fe II em. line	...	...	yes	CS dust
M31-004242.33	Of/late-WN	yes	...	...	CS nebula?
AE And	LBV	yes	...	yes	CS nebula, f-f em., H II PAH
M31-004320.97	Fe II Em. Line	yes	...	yes	CS nebula, CS dust
M31-004322.50	Warm Hypergiant	...	yes	yes	CS dust
AF And	LBV	yes	...	yes	CS nebula, f-f em., H II PAH
M31-004341.84	Of/late-WN	yes	...	yes	CS nebula, f-f em., CS dust(?)
M31-004411.36	Fe II Em. Line	yes	...	yes	CS nebula, H II PAH
M31-004415.00	Fe II Em. Line	...	yes	yes	CS dust
M31-004417.10	Fe II Em. Line	yes	yes	yes	CS dust, CS nebula
Var 15	LBV	yes	...	yes	CS nebula, H II PAH
M31-004424.21	Intermed-Type F5 Ia	yes	...	yes	CS nebula?, f-f em, H II PAH
M31-004442.28	Fe II Em. Line	...	...	yes	CS dust
M31-004444.52	Warm Hypergiant	...	yes	yes	CS dust
Var A-1	LBV	yes	...	...	CS nebula
M31-004522.58	Warm Hypergiant	yes	yes	yes	CS dust[a], CS nebula
M31-004526.62	Intermed-Type A2e Ia	yes	...	...	CS nebula, f-f em.
		M33			
Var A	Warm Hypergiant	...	yes	yes	CS dust
M33C-4174	Fe II Em. Line	yes	...	yes	CS nebula, H II PAH
M33-013242.26	Fe II Em. Line	yes	...	yes	CS nebula, H II PAH
UIT 008	Of/late-WN O7-O8f I	yes	...	yes	H II PAH
M33-013248.26	Fe II Em. Line	yes	...	yes	H II PAH
M33-013324.62	Fe II Em. Line	...	...	yes	CS dust
N045901	F I: pec	weak	...	yes	f-f em:?., CS nebula?, H II PAH
M33C-7256	Fe II Em. Line	yes	...	yes	CS nebula, CS dust
Var C	LBV	yes	...	...	CS nebula
Var B	LBV	yes	...	yes	CS nebula, H II PAH
M33C-15731	Fe II Em. Line	yes	yes	yes	CS nebula, CS dust
N093351[b]	Warm Hypergiant F0 Ia	...	yes	yes	CS dust
B324	Warm Hypergiant A8-F0 Ia	yes	yes	yes	f-f em., H II PAH
M33-013406.63	Hot Supergiant O9.5 Ia	yes	...	yes	CS nebula, H II PAH
Var 83	LBV	yes	...	...	CS nebula, f-f em.
N125093	Warm Hypergiant F0-F2 Ia	...	yes	yes	CS dust
Var 2	LBV	yes	...	...	CS nebula
M33-013426.11	Fe II Em. Line	...	yes	yes	CS dust
M33-013442.14	Intermed-Type A8 Ia	...	...	yes	CS dust
M33-013459.47	Fe II Em. Line	yes	...	yes	CS nebula, f-f em. +CS dust(?), H II PAH
M33-013500.30	Fe II Em. Line	yes	...	yes	CS nebula, CS dust
GR 290/V532	Of/late-WN	yes	...	...	CS nebula

Notes.
[a] In Paper I we noted that the IRAC photometry was discrepant and suggestive of H II contamination. The IRAC source is more than 5″ away and in H II nebulosity while the *WISE* source agrees with the position of the star.
[b] N093351 is a good example of the role of nebular contamination in the spectra from nearby emission nebulosity. The MMT/Hectospec spectrum shows strong nebular emission lines in the 1.″5 aperture while the same lines are not present in the LBT/MODS1 spectrum with a 0.″6 slit and sky subtraction immediately on either side of the star.

excess radiation from circumstellar dust. Many of the hot supergiants show weak nebular emission in their spectra due to contamination from emission nebulosity in the Hectospec aperture. Fortunately, the relative strengths of the [N II] lines (K. Weis et al. 2014, in preparation) allow us to separate a likely circumstellar nebula from an H II region. The stars with H II emission contamination in their spectra distinct from a circumstellar nebula are not included in Table 3. H II regions also contribute polycyclic aromatic hydrocarbon (PAH) and dust emission at long wavelengths (Tielens et al. 1999; Peeters et al. 1999; Draine & Li 2007). We observe this infrared emission in the SEDs of several of our stars embedded in emission nebulosity which contributes to the flux especially in the *WISE* 6″ aperture. In Figure 8 we show three examples; a normal hot supergiant, an F-type supergiant, and the LBV AE And. Except for a small free–free contribution in the near-infrared, these three stars' SEDs show no evidence of warm circumstellar dust but have associated nebular emission. It is therefore necessary to distinguish this long wavelength nebular dust emission from circumstellar dust produced by the star's own mass loss. However, many of these stars are hot and can ionize their ejecta possibly creating a compact region of ionized hydrogen near the star. We therefore inspected the Hα images (Massey et al. 2006) to look for extended nebulosity at the star's position. Combining all of this information, we distinguish the two cases, CS nebula or H II region and if the star has long

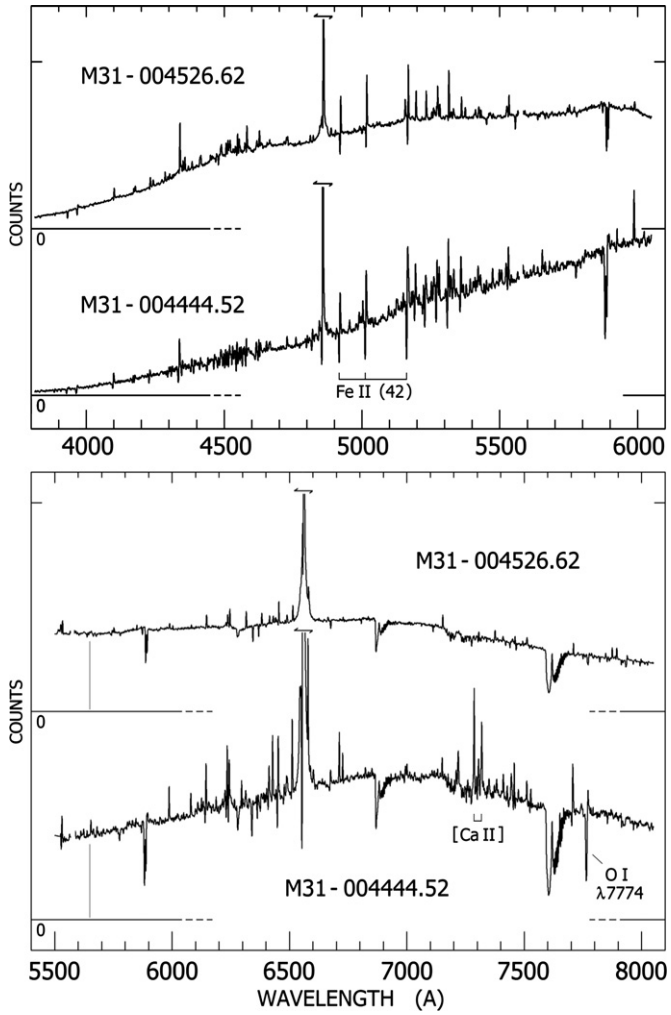

Figure 7. Blue and red MMT spectra of M31-004526.62(A2eI) and the warm hypergiant M31-004444.52(F0 Ia).

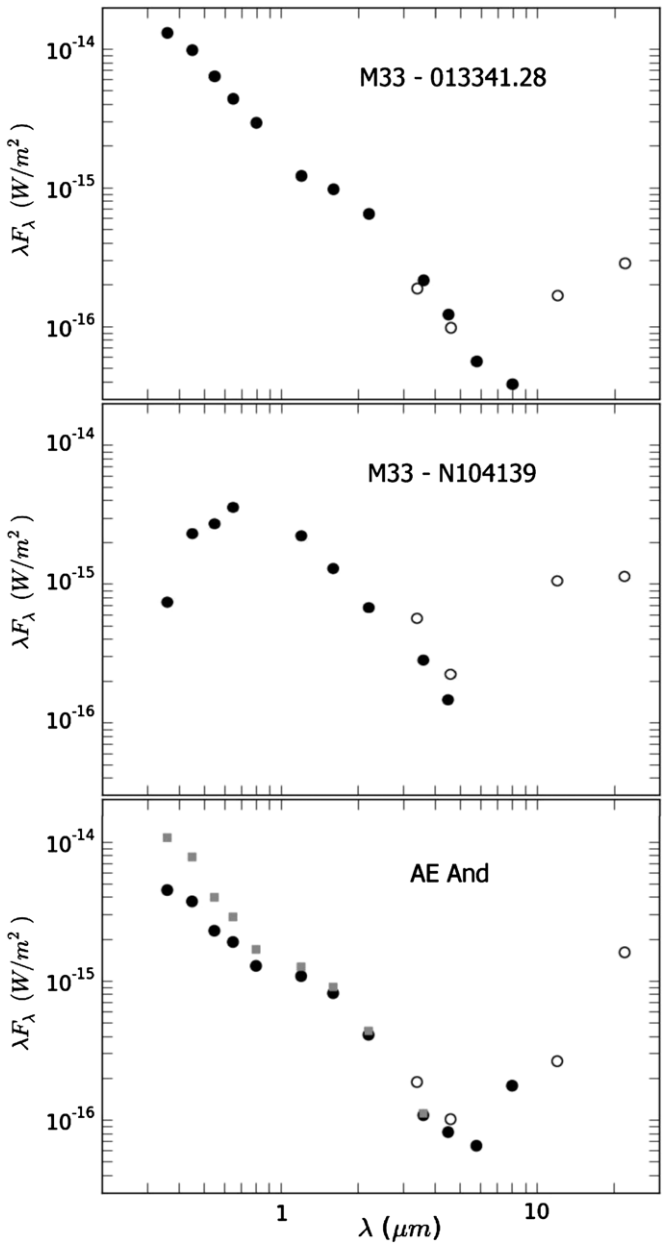

Figure 8. Examples of H II region PAH and dust emission longward of 8 μm in the SEDs of three stars; M33-013341.28, a normal hot supergiant (B2-3 Ia), M33-N104319, a normal F-type supergiant (F5 Ia), and the LBV, AE And. The observed visual, 2MASS, and IRAC magnitudes are shown as filled circles and the *WISE* data as open circles. The SEDs for the two supergiants are not corrected for interstellar extinction. The extinction-corrected photometry for AE And is plotted as filled squares.

wavelength excess radiation, we include "CS dust" or possible "H II PAH" in the comments column of Table 3.

3.1. The Spectral Energy Distributions

In addition to the evidence for circumstellar nebulae discussed by K. Weis et al. (2014, in preparation), we find that many of the stars described in Section 2 have warm circumstellar dust including several of the Fe II emission line stars, but conclude that the known LBVs do not.

To determine whether these stars have excess free–free emission from their stellar winds and/or circumstellar dust, as well as their intrinsic luminosities, we must first correct their SEDs for interstellar extinction. This is an uncertain procedure for stars with strong emission lines. Their broadband colors cannot be safely used especially in the blue-visual region. We therefore estimate the visual extinction, A_v, from other indicators including the well-known relation between the neutral hydrogen column density ($N_{\rm H\,I}$) and the color excess, E_{B-V} (Knapp et al. 1973; Savage & Jenkins 1972), and A_v from the Q-method for nearby OB-type stars within a few arcsec of the target assuming that their UBV colors from Massey et al. (2006) are normal. We use $R = 3.2$ and the standard extinction curve from Cardelli et al. (1989). The results from these different methods are summarized in Table 4; A_v defined as the foreground A_v (≈0.3 mag) plus 1/2 A_v[4] from $N_{\rm H\,I}$ from the recent H I surveys of M31 (Braun et al. 2009) and M33 (Gratier et al. 2010), A_v for several of the known LBVs from Szeifert et al. (1996) who likewise used $N_{\rm H\,I}$ from earlier H I surveys, A_v from the observed colors for the F-type supergiants, and A_v from nearby stars with the number of stars used in parenthesis. We favor the extinction estimates from nearby stars when available because of their proximity to the target stars, compared to the H I surveys which have spatial resolutions of 30″ and 17″ for

[4] Since we do not know the exact location of the stars along the line of sight with respect to the neutral hydrogen, we adopt half the extinction derived in this way.

Table 4
Extinction and Total Luminosities

Star	A_v ((H I) (mag)	A_v (H I(Seizert) (mag)	A_v (colors) (mag)	A_v (stars) (mag)	Adopted A_v (mag)	M_v (mag)	$M_{\rm Bol}$ (mag)
		M31					
AE And (LBV)	0.9	0.6	...	0.9 (1)	0.6	−7.6	−9.3 to −9.8
AF And (LBV)	1.1	1.0	...	...	1.0	−8.1	−10.7
Var A-1 (LBV)	1.9	...	...	1.5 (1)	1.5	−8.8	−10.1:
Var 15 (LBV)	1.3	...	...	0.3 (1)	1.3	−7.3	−8.5:
M31-004229.87 (Fe II em)	2.1	...	...	1.4 (2)	1.4	−7.0	−8.1:
M31-004320.97 (Fe II em)	1.5	...	...	...	1.5	−6.7	−7.8:
M31-004411.31 (Fe II em)	0.8	...	...	2.3 (3)	2.3	−8.6	−9.7:
M31-004415.00 (Fe II em)	0.9	...	...	2.7 (2)	2.7	−8.8	−9.6:
M31-004417.10 (Fe II em)	1.7	...	...	0.7 (1)	0.7	−8.0	−-8.3:
M31-004442.28 (Fe II em)	1.7	...	...	1.2 (1)	1.2	−5.9	−8.3:
M31-004526.62 (A2e Ia)	1.3	...	1.5	1.6 (1)	1.5	−8.7	−8.9
M31-004424.21 (F5 Ia)	1.9	...	1.9	1.6 (4)	1.9	−9.6	−9.5
M31-004425.18 (B2-B3 I)	0.7	...	...	...	0.7	−7.7	−8.0
		M33					
Var B (LBV)	0.3(min.)	0.7	...	...	0.7	...	−10.4
Var C (LBV)	0.4	0.85	...	0.7 (1)	0.85	−8.1	−9.8
Var 83 (LBV)	0.9	1.05	...	0.85 (2)	1.0	−9.5	−11.1
Var 2 (LBV)	1.0	...	...	0.2 (1)	1.0	−7.3	−9.1:
M33C-4174 (Fe II em)	0.9	...	...	0.8 (3)	0.8	−7.3	−8.7:
M33-013242.26 (Fe II em)	0.8	...	...	0.9 (2)	0.9	−8.0	−8.9:
M33-013248.26 (Fe II em)	0.4	...	...	0.3 (2)	0.4	−7.6	−8.9:
M33-013324.62 (Fe II em)	0.4	...	...	...	0.4	−5.3	−6.3:
M33C-7256 (Fe II em)	0.3(min)	...	...	0.5 (3)	0.5	−5.6	7.6:
M33C-15731 (Fe II em)	0.7	...	...	1.2 (2)	1.2	−8.9	−10.9
M33-013426.11 (Fe II em)	0.6	...	...	...	0.6	−6.1	−6.9:
M33-013459.47 (Fe II em)	0.7	...	...	...	0.7	−6.8	−7.5:
M33-013500.30 (Fe II em)	0.7	...	...	0.3 (3)	0.7	−5.5	−6.9:
UIT 008 (O7-O8f/WN9)	0.8	...	0.6	0.4(1)	0.6	−7.5	−10.7
M33-013406.63 (O9.5 I)	0.7(1.2)	...	1.5	0.3(2), 0.8(1)	0.7(1.2)	−9.1(−9.6)	−12.2(−12.7)
M33C-4640 (A0-A2e Ia)	0.6	...	0.4	0.65(2)	0.6	−8.1	−8.3
M33-013442.14 (A8 Ia)	1.2	...	2.1	0.45 (1)	2.1	−9.3	−9.2
M33-N045901(F I pec)	0.5	...	1.6	0.9 (1)	1.6	−8.5	−8.4
Gr290/V532 (Of/WN)	0.6	...	...	...	0.6[a]	var.	−10.4–−10.7

Note. [a] Romano's star. In addition to the estimated A_v from the H I, two nearby associations, OB 88 and OB 89 yield $A_v \approx 0.5$ mag. The star is variable. We adopt the magnitudes at visual maximum and minimum and the corresponding temperatures from Sholukhova et al. (2011) together with the bolometric corrections using the B.C discussed by Polcaro et al. (2011) for visual maximum. This yields a range for $M_{\rm bol}$ of −10.4 to −10.7 at visual maximum and −10.5 at minimum.

M31 and M33, respectively. Table 4 includes the adopted A_v and their corresponding extinction-corrected visual and bolometric luminosities with the same distance moduli used in Paper I, 24.4 mag for M31 and 24.5 mag for M33.

The SEDs for the known LBVs are shown in Figure 9; AE And is in Figure 8. LBVs are variable and understandably the broadband visual, and near- (2MASS) and mid-infrared (IRAC and *WISE*) photometry was not all observed at the same time, and therefore do not always yield SEDs corresponding to the same time frame. This is especially true for Var B and Var C which as noted in Section 2.1, have experienced LBV-type optically thick wind episodes in the past decade when these data were obtained. The visual photometry for Var C from Massey et al. (2006) is consistent with earlier *B* and *V* magnitudes (Szeifert et al. 1996). We therefore adopt the corresponding *JHK* photometry from Szeifert et al. (1996) for its SED in Figure 9. Var B is not shown here for this reason; see Figure 9 in Szeifert et al. (1996) for its SED near its visual maximum. Interestingly, comparison with the earlier photometry for M31-Var 15, shows that it declined by about one magnitude from 1992 to 2001. The visual and near-IR photometry used here for the other LBVs are consistent with the earlier observations. As we noted in Szeifert et al. (1996), the LBVs show excess near-IR radiation due to free–free emission. With the addition of the IRAC and *WISE* bands, we conclude that there is no evidence for hot or warm CS dust in the LBVs based on their SEDs in Figures 8 and 9. The SEDs of AF And, Var 15 and AE And show an increase in flux at and longward of 8 μm but no evidence of warm circumstellar dust at the shorter wavelengths. We attribute this apparent infrared excess to probable PAH and dust emission from H II nebulosity primarily in the 6″ *WISE* aperture. AE And could be a good candidate for an associated compact H II region, but close inspection of the Hα image of AE And shows a wisp of nebulosity passing through the position of the star, although it also has a dense N-rich circumstellar nebula (K. Weis et al. 2014, in preparation).

Szeifert et al. (1996) combined UV fluxes from *HST*/Faint Optical Spectrograph near-UV spectroscopy with visual and near-IR photometry for several of the M31 and M33 LBVs to estimate their corresponding bolometric luminosities and temperatures from their SEDs. We therefore adopt the A_v values from that paper and their derived bolometric luminosities,

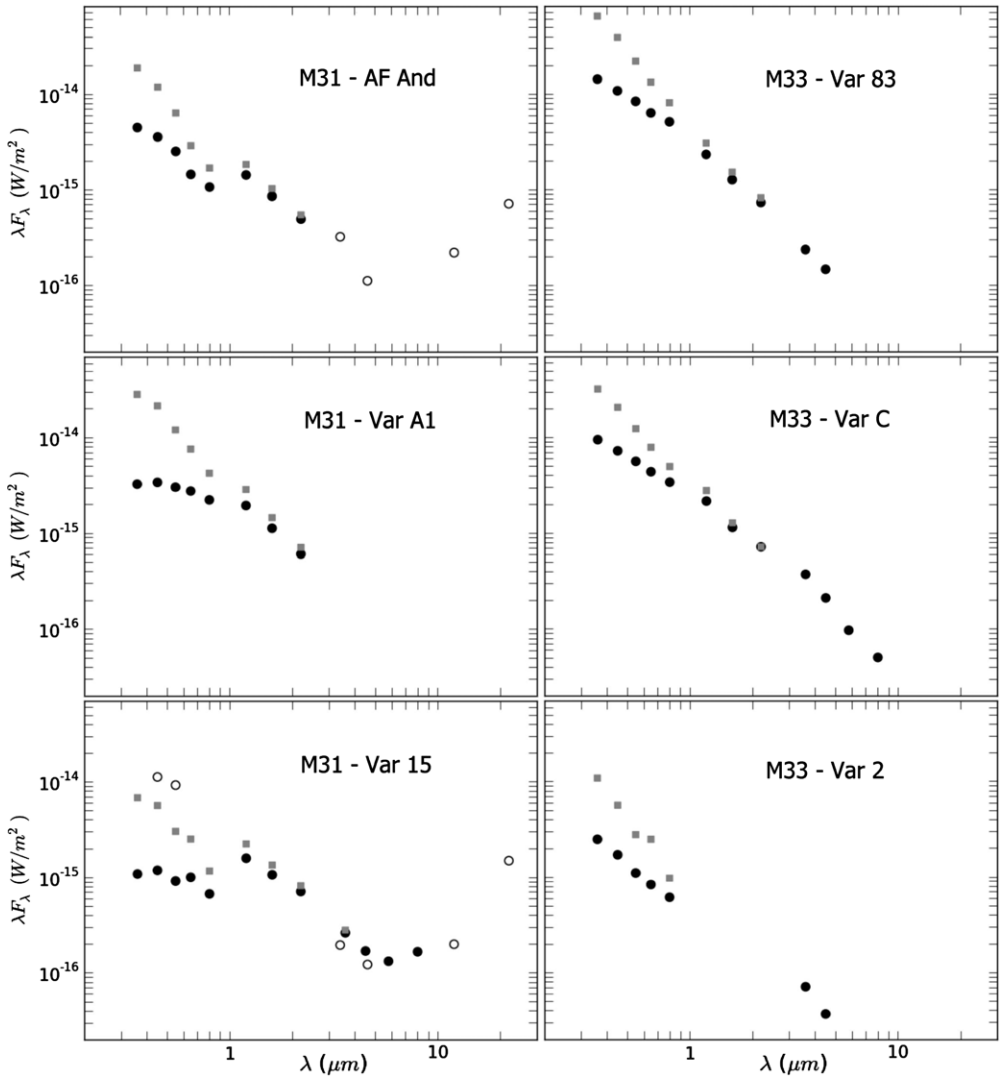

Figure 9. SEDs for the confirmed LBVs. The symbols are the same as in Figure 7, except for Var. 15. We also use open circles for the earlier B and V photometry when it was brighter. As noted in the text, we have used visual and near-infrared photometry for Szeifert et al. (1996) for Var C. Note that AF And and Var. 15 show PAH emission.

adjusted for the small change in distance moduli, for AE And, AF And, Var B, Var C, and Var 83 in Table 4.

Figures 10(a) and (b) show the SEDs for the Fe II emission line stars in M31 and M33 with long wavelength evidence for CS dust. Our criterion for concluding that these stars have circumstellar dust is based on a rise in their SEDs > 2 μm above what would be expected from an extrapolation of their visual SEDs or a contribution from free–free emission at the longer wavelengths. Due to their faintness, *JHK* photometry from 2MASS is not available for some of them, but, nevertheless, their SEDs clearly show an excess at wavelengths longward of 3 μm. The SEDs for many of these stars also show an excess in the *U* band. We note that the observed $U-B$ colors of many of the Fe II emission line stars are unusually negative, that is very blue, and even moreso when corrected for the adopted A_v values. Interestingly, this is a characteristic that they share with the LBVs and warm hypergiants. The broadband *U* magnitude is much less affected by emission lines in their spectra than the *B* magnitude wavelength range where there are numerous strong Fe II emission lines. The apparent $U-B$ color excess is thus due mostly to increased flux in the *U* band as seen in their SEDs. Given the very strong hydrogen emission lines in their spectra, we suggest that this excess *U* band flux is due to emission in the Balmer continuum below 3600 Å. The *R* band flux is also elevated in several of the SEDs due to the very strong Hα emission line. The SEDs for M33C-15731 (UIT 212) and M33-013406.63 (UIT 301) which have additional NUV and FUV flux measurements (Massey et al. 1996) are shown in Figure 10(c).

The long wavelength SEDs of the Fe II emission line stars are complex including free–free emission and scattered light from warm dust in the near-infrared, and thermal emission longward of 3.5 μm. M33C-15731 in Figure 10(c) is a good example. We used the LMC average extinction curve from Gordon et al. (2003) to correct its NUV and FUV fluxes. Earlier work (Szeifert et al. 1996, and references therein) had found that the LMC UV extinction curve was more appropriate for the massive stars in M31 and M33. The addition of the short wavelength fluxes allow us to estimate a temperature based on a 21,400 K blackbody fit through its UV and visual fluxes. Its SED also illustrates the *U* band excess, the near-IR free–free emission, and additional excess radiation at the longer wavelengths.

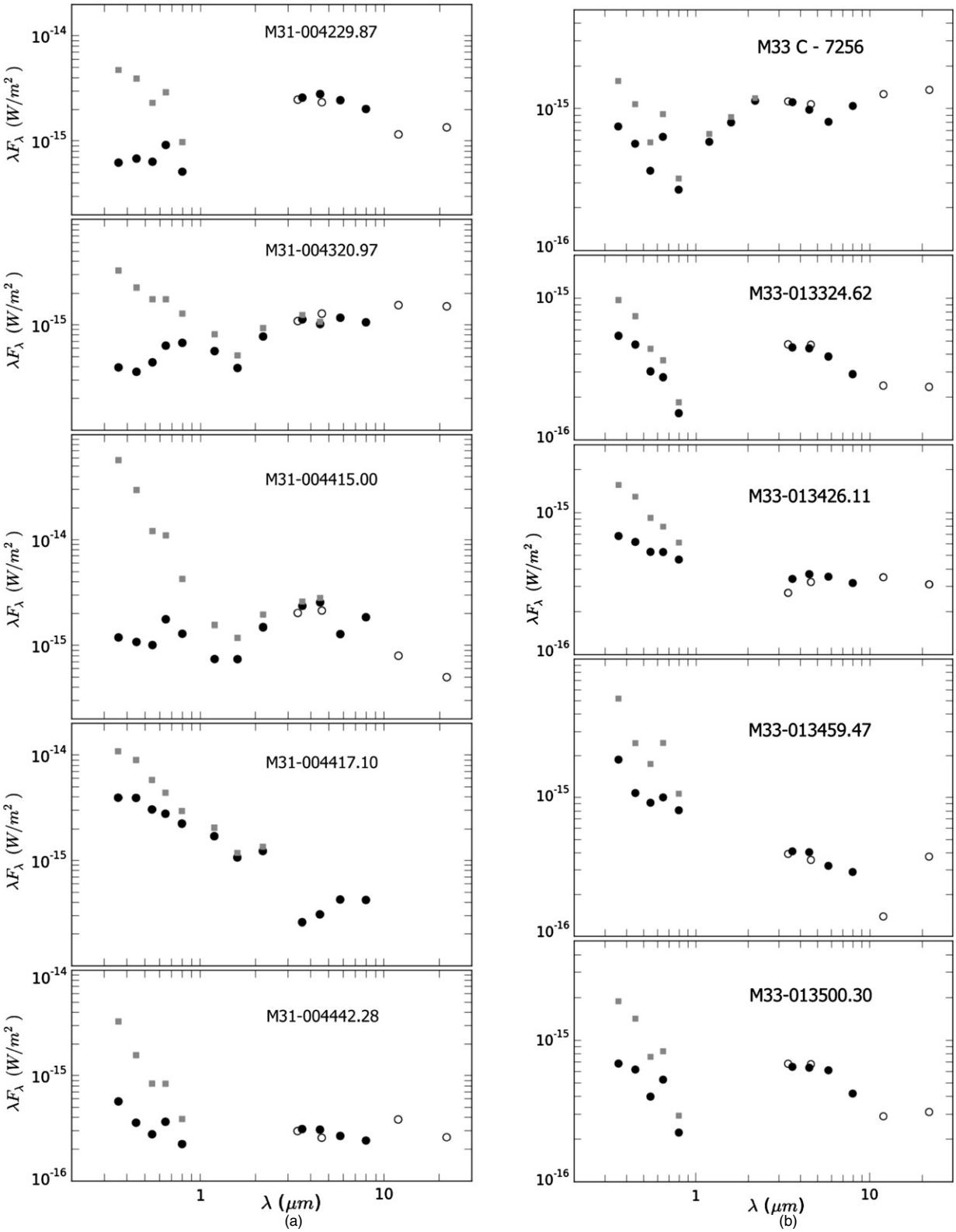

Figure 10. (a) The SEDs for five Fe II emission line stars in M33 with circumstellar dust. The symbols are the same as in Figure 7. (b) The SEDs for five Fe II emission line stars in M33 with circumstellar dust. The symbols are the same as in Figure 7. Although M33-013459.47 shows the characteristic PAH upturn, it is shown here because its SED shows an excess at 3 to 8 μm; its infrared excess is very likely due to a combination of free–free emission, some CS dust with a contribution from H II region PAH emission. (c) The SEDs for M33C-15731 and M33-013406.63. The symbols are the same as in Figure 7 with the addition of open squares for the second extinction correction for M33-013406.63 discussed in the text. The NUV and FUV fluxes are from the 1500 Å and 2400 Å magnitudes from the UIT survey (Massey et al. 1996) and transformed to fluxes following the prescription in that paper. They were corrected for interstellar extinction using the adopted A_v and the average extinction curve for the LMC for these UV wavelengths (Gordon et al. 2003). Like the SEDs for the LBVs (Szeifert et al. 1996), they show the dip at 2000–2400 Å, and have an excess in the *U* band most likely due to Balmer continuum emission. A 21,400 K blackbody is shown fit through M33C-15731's blue-visual and 1500 Å broadband points. The near-IR free–free emission and the presence of dust >3.5 μm are apparent. M33-013406.63 is shown corrected for values of A_v, 0.7 mag and 1.2 mag discussed in the text. M33-013406.63 shows free–free emission in the near-IR, the PAH signature, but no circumstellar dust. A 30,000 K blackbody is shown through the upper points.

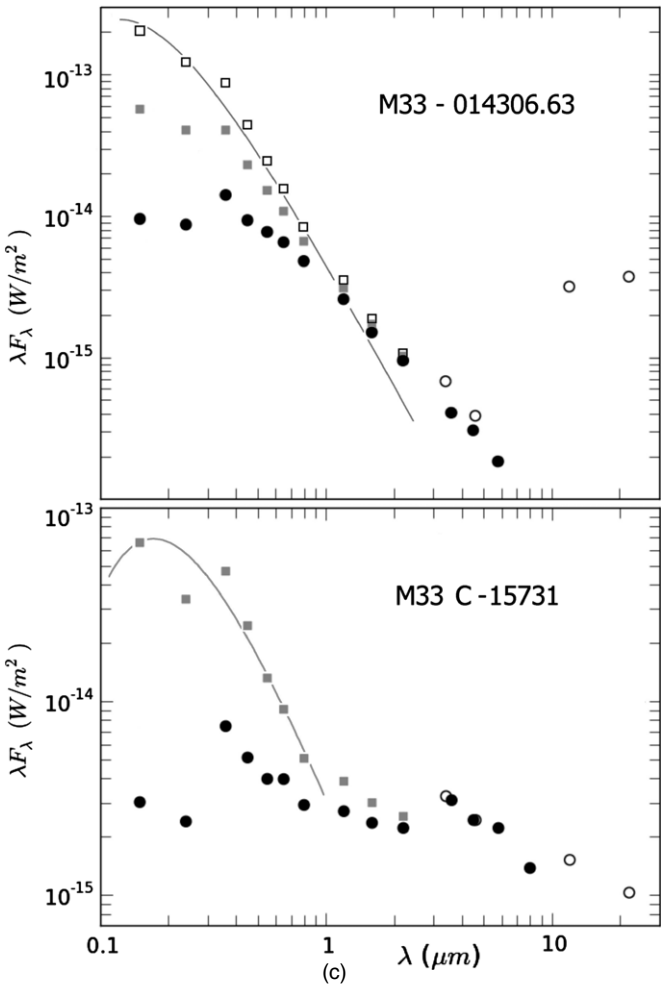

Figure 10. (Continued)

M33-013406.63 (B526/UIT 301) is embedded in a prominent H II region. Its SED, also shown in Figure 10(c), has a significant excess at long wavelengths most likely due to PAH emission from the surrounding H II region, but no evidence for hot or warm circumstellar dust. Based on its O9.5 Ia spectral type, we would expect a temperature near 30,000 K (Martins et al. 2005; Massey et al. 2004). With the adopted A_v of 0.7, however, it is clear that a 30,000 K blackbody is not a good fit to the SED, and a significantly lower temperature ≈20,000 K is implied. The discrepancy is most likely due to the uncertainty in the visual extinction correction. The SED is more consistent with the expected temperature with a higher A_v of 1.2 mag, the maximum value from the neutral hydrogen column density. An A_v as high as 1.5 mag is even suggested based on its observed $B-V$ color, although the color may be affected by its strong hydrogen emission. With this possible range in the visual extinction, M33-013406.63's visual luminosity is M_v is −9.1 to −9.6 mag and with a bolometric correction of −3.1 corresponding to is apparent spectral type, its bolometric luminosity is −12.2 to −12.7 mag, exceeding the luminosity of η Car. M33-013406.63 is very likely a binary or multiple star, but in any case, it is a very luminous star and is discussed further in Section 4.

None of the other Fe II emission line stars in M33 have UV fluxes from the UIT survey. We identified four of the M31 stars in the GALEX survey, but only one, M31-004442.28, was measured in both the NUV and FUV bands.

Without temperature indicators in their spectra together with the uncertainty in their extinction corrections, the bolometric corrections are uncertain for the other Fe II emission line stars. Except where noted, their bolometric luminosities listed in Table 4 are based on integrating their SEDs from 0.35 to 22 μm. Five of these stars show a significant contribution to their SEDs from circumstellar dust and to their total luminosities, even when we consider the possibility that the visual extinction corrections may have been underestimated and the stars are actually visually brighter. For the other stars, the dusty contribution is at a relatively low level. In all cases the circumstellar dust appears to be fairly warm. Longward of 2–3 μm, the relatively flat SEDs suggest a range of dust temperatures from a few 100 to 1000 K. Based on their visual SEDs and the presence of He I emission in some of their spectra, many of these stars are fairly warm, but without information on their UV fluxes the bolometric luminositites in Table 4 are very likely under estimates for most of the Fe II emission line stars. For M33C-15731 we assumed the temperature from the blackbody fit (Figure 10(c)) plus the contribution from free–free emission and dust, and for M33-013406.63 we use the inferred temperature and bolometric correction corresponding to its spectral type with the range of extinction corrections discussed above.

The SEDs for three intermediate-type supergiants discussed in Section 2.5 are shown in Figure 11. The adopted visual extinction corrections for these stars is based on their observed colors. Their blue-visual colors are not seriously compromised by the emission lines in their spectra, and the A_v values from the different methods in Table 4 are consistent, although for M33-013442.14 only one nearby star is available for comparison, and the maximum A_v from $N_{\rm H\,I}$ would be 2.1 mag, equal to the A_v from its colors. It also has CS dust which could contribute to its extinction. We used the bolometric correction appropriate to the spectral types for the two stars in M31 and integrated the SED for M33-013442.14 even though the contribution from its long wavelength excess is small. We note that all three of these stars which show evidence for CS nebulosity, ejecta, and winds are quite luminous.

We mention N045901 here and include it in Tables 3 and 4 because it has been proposed as a possible LBV candidate but as we emphasized in Section 2.5 that suggestion is not supported by its spectrum. Cross-identification with possible 2MASS and IRAC sources is also doubtful, see the notes to Table 2. Thus there is no convincing evidence for circumstellar ejecta.

3.2. Circumstellar Nebulae, Winds, and Outflows

P Cyg profiles, asymmetric profiles, broad wings, and double or split hydrogen emission lines, are all indicators of winds, mass loss and outflows. Most of the stars in our program, the hot supergiants, the WR stars, as well as the LBVs, show prominent P Cygni profiles in the hydrogen emission lines. These stars all have winds and mass loss. Consequently, in this section we will focus on the evidence for circumstellar nebulae and gaseous outflows in the LBVs, the Fe II emission line stars, and some of the intermediate-type stars of interest.

Using the ratio of the [N II] nebular emission lines λ5755/λ6584, in the spectra of our luminous stars, K. Weis et al. (2014, in preparation) found that most of the known LBVs, several candidates, and Fe II emission line stars have electron densities on the order of 10^6 cm^{-3} or higher, much greater than for an H II region, suggesting the presence of circumstellar nebulosity. These stars are included in our Table 3 with CS nebula in the

Table 5
Outflow Velocities (km s^{-1})

Star	P Cyg (H)	P Cyg (He I)	P Cyg (Fe II)	Double Hα
		LBVs		
AE And(B2-3)	−151(2) ± 2.0	−161(2) ± 4.0	...	...
AF And(Of/WN)	−245(3) ± 4.5	−222(4) ± 4.6	−213([Fe III])(2) ± 2.0	...
Var 15(Of/WN)	−219(4) ± 3.1	−205(6) ± 10	...	...
Var A-1	−200(4) ± 2.8	−160(2) ± 5.0	−219(1)	...
Var C(B1-2, quiescence)	−158(4) ± 8	...	−157(3) ± 3	...
Var B(B0-B1)	−230(2) ± 3.0	−221(3) ± 2.7	...	...
Var 83	−158(4) ± 6.8	...	−147(3) ± 3.0	...
Var 2(Of/WN)	−221(1)	−236(4) ± 4.1	...	...
		Fe II Em. Line		
M31-004415.00	...	...	...	−120,+155
M31-004417.10	...	−269(1)	...	...
M33C-4174	...	−168(1)	...	...
M33C-15731	−216(3) ± 8.0	...	...	...
M33-013426.11	−242(2) ± 5.7	...	...	...
		Warm Hypergiants[a]		
M31-004322.50(late A-F0)[b]	−240(1)	...	−185(3) ± 3	...
M31-004444.52(F0 Ia)[b]	−244(3) ± 2	...	−214(3) ± 9	...
M31-004522.58(A2 Ia)	...	...	...	±100
N093351(F0 Ia)	−127(1)	...	...	±120
B324(A8-F0 Ia)[b]	−143(1)	...	...	...
N125093(F0-F2 Ia)	−262(1)	...	...	±220
		Other Stars (Table 4)		
GR 290/V532(Of/WN - 2010)	...	−234(4) ± 5.0	...	
M33-013406.63(O9.5 Ia)	...	−307(1)	...	...
M31-004526.62(A2e Ia)	−146(4) ± 4.6	...	−139(3) ± 2.5	...
M33-013442.14(A8 Ia)	−221(2) ± 8.2			
UIT 008(O7-O8/WN9)	−159(1)	−138(1)	...	...
M31-004425.18(B2-B3 I)	−153(3) ± 8.9	...	...	...
N045901(F: I)	...	...	...	±90
		Normal Supergiants		
Of/late-WNs(9 stars)	−329(7) ± 23	−313(20) ± 15.6	...	...
Early B(B0-B3)(12 stars)	−220(15) ± 5	−213(9) ± 9	...	...
Late B(B5-B8)(13 stars)	−161(19) ± 7	−160(3) ± 3.4	...	...
A type(A0-A8)(6 stars)	−142(9) ± 5.4	...	...	...

Notes.
[a] The velocities for the warm hypergiants (Paper I) are repeated here for completeness and due to wavelength calibration problems with the LBT spectra which have been corrected here.
[b] P Cyg velocities for the Ca II[Ca II] profiles, M31-004322.50: −90, M31-004444.52: −200, B324: −126.

remarks column. Three of the four Fe II emission line stars with [Ca II] in emission (Section 3.2) also have [N II] ratios indicative of a circumstellar nebula. For comparison, the [Ca II]/Ca II ratio for M33C-15731 and M31-004417, yield higher densities of 5–6 × 10^7 cm^{-3} which are also somewhat higher than we found for the warm hypergiants in Paper I.

It is customary to measure the wind speed or terminal velocity (v_∞) from the blue edge of the P Cygni profile, but for these moderate resolution spectra, and especially for the stars with poorer S/N and poorly defined continua, the absorption minimum provides a more well-defined differential measurement. The stars with P Cygni profiles in their hydrogen, He I, and/or Fe II emission lines are listed in Table 5 with their outflow velocities measured from the absorption minima in their P Cygni profiles relative to the emission line peak. The outflow velocities from the double H emission lines when present in a few stars are also given. For those spectra with good S/N, such as Var C in M33, the results from the absorption minimum are consistent with and parallel the behavior of the terminal or blue-edge velocity (Humphreys et al. 2014). For comparison, the wind speeds from the P Cygni profiles in the normal supergiants in M31 and M33 measured the same way are also included in Table 5.

LBVs are well-known to have low wind speeds of 100–200 km s^{-1} during their eruptions or maximum light phase. We find that the known LBVs in M31 and M33 also have relatively low outflow velocities even in their quiescent phase. The outflow velocities of these LBVs in quiescence are typically 50–100 km s^{-1} less than for the normal supergiants in our sample with similar spectral types. For example, the outflow velocities of the LBVs with early B-type spectra in their quiescent or hot state average −170 km s^{-1} compared to −220 km s^{-1} for the normal supergiants. Similarly, the three LBVs with Of/WN type spectra have wind velocities typically 100 km s^{-1} less than the average for the Of/WN stars in our sample. GR290, Romano's star, shows the same difference. Although wind speeds are expected to have some dependence on metallicity, we do not find any significant difference in the wind velocities between the M31 and M33 LBVs in this small sample or between the normal supergiants in the two galaxies. This is not surprising given the range in the measured velocities and their associated measured uncertainties.

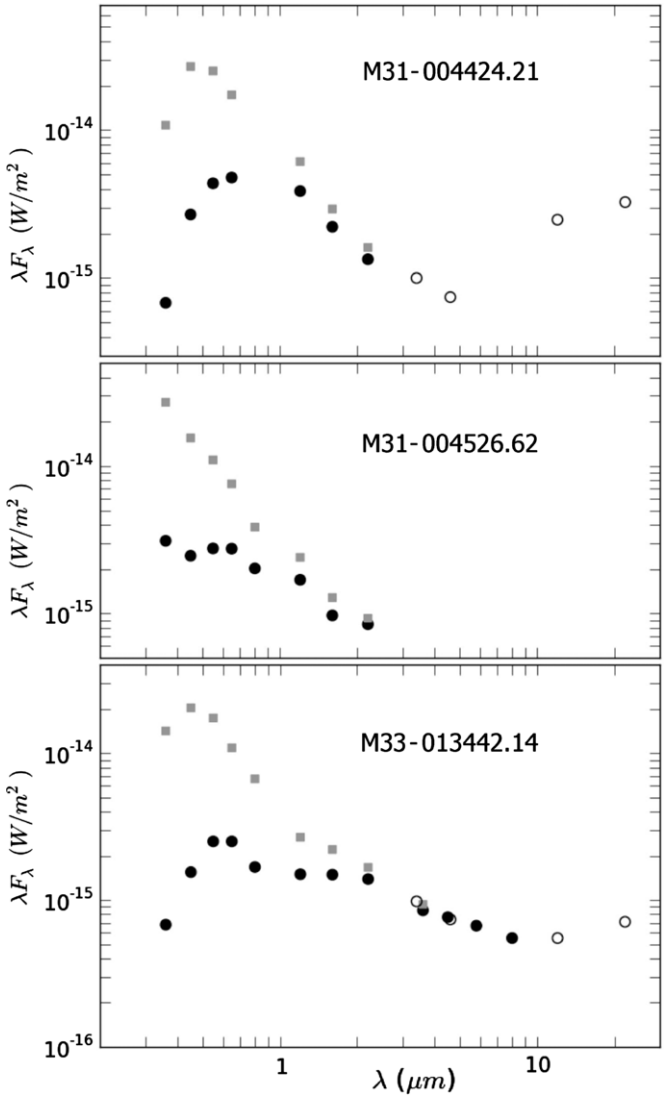

Figure 11. SEDs for three of the luminous F-type supergiants. M33-013442.14 has excess radiation from both free–free emission in the near-infrared and from dust at the longer wavelengths. M31-004424.21 shows PAH emission.

The well-studied Galactic LBV, AG Car, similarly has a relatively low terminal velocity during its quiescent or hot stage when it is spectroscopically like an Of/late WN-type star (WN11 Smith et al. 1994). Its terminal velocity, measured from the blue-edge (Leitherer et al. 1994; Stahl et al. 2001; Groh et al. 2009), is 250 to 300 km s^{-1}. Groh et al. (2009) reported an even lower velocity of 105 km s^{-1} during its 2001 minimum or quiescent state, although it had not returned to it previous high temperature. These wind velocities are low compared to terminal velocities of 400–1300 km s^{-1} for the Of/late-WN stars and WNL stars (Crowther et al. 1995a, 1995b) and 400 to 1000 km s^{-1} for Galactic and LMC early-type supergiants (Crowther et al. 2006; Mokiem et al. 2007).

Thus, the winds of the LBVs even in their hot, quiescent state are apparently slower and presumably denser than the normal hot supergiants with similar spectroscopic temperatures. This should not be surprising. LBVs are presumably close to their Eddington limit (Humphreys & Davidson 1994). They have lost much of their mass in previous S Dor-type maxima or even in a previous giant eruption. Thus their effective gravities and escape velocities are now much lower.

Table 6
Mass Lost Estimates

Star	Mass Lost ($M_\odot$) IR (SED)
M31-004229.87 (Fe II em.)	1.82×10^{-2}
M31-004320.97 (Fe II em.)	0.95×10^{-2}
M31-004415.00 (Fe II em.)	1.66×10^{-2}
M31-004417.10 (Fe II em.)	0.38×10^{-2}
M31-004442.28 (Fe II em.)	0.22×10^{-2}
M33-013324.62 (Fe II em.)	0.92×10^{-2}
M33C-7256 (Fe II em.)	0.56×10^{-2}
M33C-15731 (Fe II em.)	1.40×10^{-2}
M33-013426.11 (Fe II em.)	0.32×10^{-2}
M33-013442.14 (A8 Ia)	0.56×10^{-2}
M33-013459.47 (Fe II em.)	0.29×10^{-2}
M33-013500.30 (Fe II em.)	0.42×10^{-2}

3.3. Circumstellar Dust and Mass Lost Estimates

The 3.5 μm to 8 μm fluxes from the IRAC data clearly show the presence of dusty circumstellar ejecta in the SEDs for several of stars discussed in this paper, and the *WISE* data indicate that the thermal emission extends to even longer wavelengths in several cases. We can estimate the mass of the circumstellar ejecta from the flux at mid-infrared wavelengths using the equation for the dust mass and following the prescription in Paper I with the flux at 8 μm and an assumed grain temperature of 350 K at that wavelength. The results are in Table 6.

Overall, the mass in the ejecta ranges from a high of about two times 10^{-2} to a few times 10^{-3} $M_\odot$. The highest values for the Fe II emission line stars are comparable to our estimates for the warm hypergiants in Paper I, but overall, they average somewhat lower.

4. SUMMARY AND CONCLUDING REMARKS

In this section we summarize our results for the LBVs, other variables, the Fe II emission line stars, the intermediate-type supergiants with comments on post-red supergiant evolution, and the very luminous M33-013406.63 (B416, UIT301). The stars discussed in this section are shown on an HR Diagram in Figure 12.

4.1. The Luminous Blue Variables

We find that the confirmed LBVs have low wind speeds in their hot, quiescent or visual minimum state, compared to the B-type supergiants and Of/WN stars which they spectroscopically resemble. In the case of Var C, currently in eruption (Humphreys et al. 2014), there is little difference in the outflow velocities between the two states. The lower wind speeds and presumably denser winds, even in quiescence, may be another distinguishing property of the LBV/S Dor variables and consequently may aid in identifying candidates in addition to the characteristic, but infrequent, S Dor variability. This may be a significant clue to the structural trait that causes the LBV instability. Due to their record of higher-mass loss episodes, LBVs may be close to their effective Eddington limit which will result in lower escape velocities and outflow speeds.

Although many of the confirmed LBVs have circumstellar nebulosity (K. Weis et al. 2014, in preparation), we find no evidence for associated hot or warm dust although we cannot rule out the possibility of cold dust at much longer wavelengths. Oksala et al. (2013) emphasized that the LBVs in the Magellanic Clouds also lack hot dust and Kraus et al. (2014) concluded the same for two LBVs in M31. Most of the confirmed LBVs in

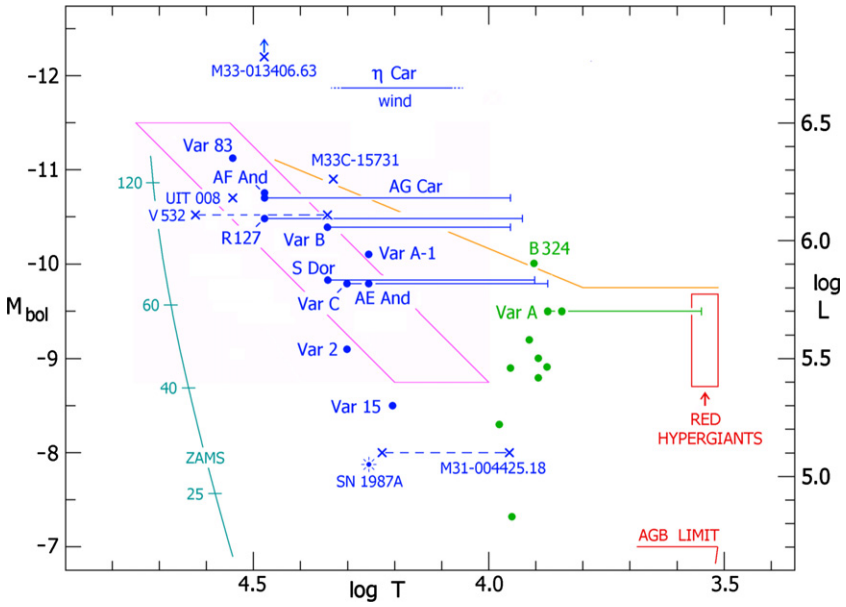

Figure 12. Schematic upper HR Diagram with the locations of the confirmed LBVs (blue dots), the warm hypergiants (Paper I) and candidate post-red supergiants (green dots), and other stars discussed in Section 4 (blue ×'s). The outline of the LBV/S Dor instability strip (pink) and the empirical upper luminosity boundary (gold) (Humphreys & Davidson 1994) are also shown. The LBV/S Dor transits to the cool dense wind state are shown as solid blue lines and those for V532/GR290 (Romano's star) and M31-004425.18 are dashed blue lines. The positions of η Car and the well-studied Galactic and LMC LBVs, AG Car, S Dor, and R 127 are shown for comparison. The apparent temperatures of Var 2, Var 15 and Var A-1 are estimates and their positions on the HRD are uncertain. Note that the solid blue transit line for Var C passes through the position of AE And.

(A color version of this figure is available in the online journal.)

the LMC and SMC also show a lack of warm dust in the 3.5 to 8 μm region (see Bonanos et al. 2009, 2010).

In addition to their unique spectroscopic and photometric variability, LBV/S Dor variables in quiescence or their hot, minimum light stage, define or lie on the "LBV/S Dor instability strip" in the upper HR Diagram (Wolf 1989; Humphreys & Davidson 1994). Most stars that lie in this locus on the HR Diagram however are *not* LBVs. Normal hot supergiants are also found in the S Dor strip.

The Of/WN star, UIT 008 in M33 has an unusually slow wind speed (Table 5) for this type of star, and thus may be an example of star that has shed a lot of mass. Its very high temperature corresponding to its O7–O8 spectral type of ≈35,000 K (Martins et al. 2005; Massey et al. 2004) and bolometric luminosity of −10.7 place it near the top of the S Dor instability strip near stars like AG Car and AF And. On this basis, it may be a candidate LBV and a star worth watching although it is not a known variable.

4.2. Other Variables

Romano's star (GR290/V532) is often called an LBV, but it does not exhibit S Dor transits to the cool, dense wind state. Instead, it varies between two hot states on the HR Diagram (Figure 12)[5] characterized by WN spectroscopic features. It also shares the lower wind speeds of the LBVs (Table 5). Given its shared characteristics with the LBVs plus its strong WR spectroscopic characteristics, we propose that Romano's star is likely in a post- LBV/S Dor state also suggested by Polcaro et al. (2011).

In Section 2.4 we suggested that M31-004425.18 may be an LBV candidate based on the evidence for a spectroscopic transition from an apparent early A-type supergiant to an early B-type. Additional confirming observations will be needed, although, like UIT 008, M31-004425.18 also has a slow wind of −153 km s^{-1} for an early B-type supergiant (Table 5). We have also estimated its luminosity (Table 4) with an extinction correction from the neutral hydrogen column density. Adopting the photometry from Massey et al. (2006) and assuming that it applies to the early A-type spectrum, we find an M_v of −7.7 mag and $M_{\rm Bol}$ of −8. Its position is shown on the HR Diagram (Figure 12) with its apparent shift to the warmer early B-type spectrum. M31-004425.18 has a rather low luminosity compared to the other LBVs and even falls below the lower limit of the less luminous LBVs on the HR Diagram.

4.3. The Fe II Emission Line Stars

One of the questions we wanted to address is the possible relation of the luminous Fe II emission line stars to LBVs, or to the LBV stage, and to the warm hypergiants. Based on the available data, the confirmed LBVs in M31 and M33 do not have significant circumstellar dust. In contrast, several of the Fe II emission line stars have both circumstellar dust and nebulosity indicative of past or present mass loss (Tables 3 and 6). Unlike LBVs in quiescence their spectra do not have absorption lines typical of hot supergiants or late WN-type stars.

M33C-15731 (UIT 212) is the most luminous Fe II emission line star. Its luminosity of $M_{\rm bol} \approx -10.7$ mag (Table 4) places it the realm of the evolved hot supergiants on the upper HR Diagram. It also has a circumstellar nebula (K. Weis et al. 2014, in preparation). With our temperature estimate from its SED (Figure 10(c)) of ≈21,000 K, M33C-15731 will fall to the right of the S Dor instability strip. Given the uncertainties in these estimates, it thus may qualify as a candidate LBV except for its dusty ejecta not shared with the known LBVs.

As discussed in Section 3.1, without absorption lines in their spectra or other information, the temperatures of most of the Fe II emission line stars are unknown. Our estimates of their

[5] See Table 4 for its extinction and luminosity estimate.

luminosities (Table 4), however, shows that most of them lie below the constant luminosity portion of the upper luminosity boundary for evolved stars in the HR Diagram (Figure 12). They have luminosities similar to the less luminous LBVs (Humphreys & Davidson 1994). Several have dusty circumstellar ejecta. The Ca II and [Ca II] emission lines in four of them, is a characteristic shared with the warm hypergiants (Paper I) and with some B[e] supergiants, although not all of our Fe II emission line stars have [Fe II]. Aret et al. (2012) reported Ca II and [Ca II] emission in the spectra of eight B[e] supergiants in the Magellanic Clouds, and noted their spectroscopic similarities to the yellow hypergiants. They suggested that those in the less-luminous regime may be candidates for blueward evolution from the yellow hypergiant phase.

Oksala et al. (2013) concluded that the C^{12}/C^{13} ratio in the CO emission features, in many sgB[e] stars support an evolved, post-main sequence state in a likely pre-red supergiant stage. However, the less luminous ones and several of the high luminosity sgB[e] stars do not show the CO emission feature, leaving their evolutionary state uncertain. In a recent review of high angular resolution observations of know sgB[e], de Wit et al. (2014) conclude that the stars in their sample have rotating equatorial disks, and several are identified with short-period binaries. They favor a pre-red supergiant phase for the sgB[e] stars. Although the evolutionary state of the sgB[e] stars is still somewhat ambiguous, there is consensus that they are in post-main sequence state and at least some of them are apparently pre-red supergiants and therefore probably not related to the LBVs. Given that Fe II emission is so common among the luminous stars, this situation is not surprising.

4.4. The Intermediate-type Supergiants and Post-red Supergiant Evolution

Blue to red evolution across the upper HR Diagram, from the end of the main sequence to the red supergiant stage and possibly back to warmer temperatures is expected to be relatively rapid. Consequently, there are not many known luminous yellow or intermediate-type supergiants. Furthermore, there is increasing evidence that massive stars above about 20 $M_{\odot}$ may not end their lives as Type II SNe in the red supergiant stage, but instead evolve back across the HR Diagram to warmer temperatures before the terminal explosion, see Paper I. Criteria for identifying and separating these post-red supergiants from normal redward evolving yellow supergiants however are uncertain.

In Paper I, we suggested that a small group of warm hypergiants with dusty circumstellar ejecta were candidates for post- red supergiant evolution. In this second paper we have classified several additional late A- and F-type supergiants. The three most luminous show evidence for circumstellar nebulosity, dusty ejecta, and mass loss, properties not shared by the other A and F-type supergiants in our sample. M33-013442.14 (A8 Ia) has circumstellar dust and strong hydrogen P -Cyg profiles (Figures 6 and 11), M31-004424.21 (F5 Ia) has circumstellar nebulosity, and M31-004526.62 (A2e Ia) closely resembles the warm hypergiant M31-004444.52 spectroscopically, with strong P Cyg profiles in the Balmer and Fe II emission lines plus circumstellar nebulosity, although it lacks the Ca II and [Ca II] emission and does not have a known infrared excess. We suggest that these stars with evidence for past and current mass loss like the warm hypergiants, may also be candidates for post-red supergiant evolution.

One additional star, M33C-4640, a less luminous A-type supergiant with weak Fe II emission, may also be a post-red supergiant candidate, but without any evidence for past or current mass loss.

4.5. A Very Luminous Star in M33

M33-013406.63 (B416, UIT 301) is a proposed LBV or LBV candidate (Shemmer et al. 2000; Fabrika et al. 2005). Its spectrum shows weak Fe II and [Fe II] emission, with strong Balmer emission and He I emission. The only P Cygni profile is observed in the λ5876 He I line. It also has absorption lines of Si IV, N III, and He II at λ4200 Å. Consequently, we suggest an O9.5 Ia classification.

It appears to be one of the most luminous stars in M33. Based on our discussion of its SED (Figure 10(c)) and interstellar extinction (Table 5), its $M_{\rm Bol}$ is −12.2 to −12.7 mag. Low amplitude photometric and small spectroscopic variability have been reported by Shemmer et al. (2000) and Sholukhova et al. (2004). On the basis of this variability, Shemmer et al. (2000) suggested that it is an LBV, while based on radial velocity variations, Sholukhova et al. (2004) propose that it is a B[e] star in a close interacting binary with a 16.1 day period. Interestingly, though, the Hα and He I λ 5876 emission lines do not vary in phase.

Given its very high luminosity, it is not surprising that M33-013406.63 may be a binary or even a multiple star system. Assuming a single star, its luminosity, $\geqslant 5.9 \times 10^6$ $L_{\odot}$, and corresponding spectroscopic temperature, ≈30,000 K, will place it far above the LBV/S Dor instability strip on the HR Diagram. If we assume two equal mass stars in the system, their luminosities would be $\approx 3 \times 10^6$ $L_{\odot}$, comparable to η Car for each. With a higher mass ratio, the primary's luminosity would exceed η Car.

M33-013406.63 is also near the center of a ring-shaped bright H II region in M33. It is tempting to speculate about its possible association with the origin of this nebula. But the H II region's linear dimensions of 104 pc by 81 pc at the distance of M33 plus the lack of the [N II] λ5755 line (Shemmer et al. 2000) in the H II region spectrum precludes the possibility that it is the remnant of a circumstellar nebula now being ionized by M33-013406.63 and other hot stars. The star itself, however, does have a circumstellar nebula (K. Weis et al. 2014, in preparation). We conclude that M33-013406.63 is not an LBV/S Dor variable but a very luminous star or pair of stars.

4.6. Concluding Remarks

In this first report on our survey of the luminous stars in M31 and M33, we have concentrated on massive stars with a known or a suspected history of mass loss, and circumstellar ejecta as revealed by their spectra and photometric histories. Based on the above discussion, we have identified three possible LBV candidates (UIT 008, M31-004425.18, and M33C-15731), and some candidates for post-red supergiant evolution. The nature of the Fe II emission line stars, at least those included here, is still uncertain, but many of them have dusty circumstellar ejecta, which separates them from the known LBVs. The very luminous late O-type supergiant, M33-013406.63, is not an LBV, but is one of the most luminous stars or pair of stars, if not the most luminous, in M33.

Subsequent papers will include additional spectra for a larger set of luminous star candidates to be followed by a summary and discussion of the luminous star populations in the upper HR diagrams of M31 and M33 and other galaxies.

Research by R. Humphreys and K. Davidson on massive stars is supported by the National Science Foundation AST-1109394. We thank David Thilker for providing a copy of their H I column density map of M31 (Braun et al. 2009). This paper uses data from the MODS1 spectrograph built with funding from NSF grant AST-9987045 and the NSF Telescope System Instrumentation Program (TSIP), with additional funds from the Ohio Board of Regents and the Ohio State University Office of Research. This publication also makes use of data products from the *Wide-field Infrared Survey Explorer*, which is a joint project of the University of California, Los Angeles, and the Jet Propulsion Laboratory/California Institute of Technology, funded by the National Aeronautics and Space Administration.

Facilities: MMT (Hectospec), LBT (MODS1)

REFERENCES

Arellano Ferro, A., Giridhar, S., & Rojo Arellano, E. 2003, RMxAA, 39, 3
Aret, A., Kraus, M., Muratore, M. F., & Borges Fernandes, M. 2012, MNRAS, 423, 284
Bonanos, A. Z., Lennon, D. J., Köhlinger, F., et al. 2010, AJ, 140, 416
Bonanos, A. Z., Massa, D. L., Sewilo, M., et al. 2009, AJ, 138, 1003
Bond, H. E. 2011, ApJ, 737, 17
Braun, R., Thilker, D. A., Walterbos, R. A. M., & Corbelli, E. 2009, ApJ, 695, 937
Burggraf, B. 2014, PhD thesis, Univ. of Bochum
Burggraf, B., Wejs, K., Bomans, D. J., et al. 2014, A&A, submitted
Cardelli, J. A., Clayton, G. C., & Mathis, J. S. 1989, ApJ, 345, 245
Clark, J. S., Castro, N., Garcia, M., et al. 2012, A&A, 541, A146
Conti, P. S., & Massey, P. 1981, ApJ, 249, 471
Crowther, P. A., Hillier, D. J., & Smith, L. J. 1995a, A&A, 293, 172
Crowther, P. A., Hillier, D. J., & Smith, L. J. 1995b, A&A, 293, 403
Crowther, P., Lennon, D. J., & Walborn, N. R. 2006, A&A, 446, 279
Cutri, R. M., Skrutskie, M. F., Van Dyk, S., et al. 2003, The IRSA 2MASS All-Sky Point Source Catalog, NASA/IPAC Infrared Science Archive
de Wit, W.J, Oudmaijer, R. D., & Vink, J. S. 2014, AdAst, 2014, 10
Draine, B. T., & Li, A. 2007, ApJ, 657, 810
Drout, M. R., Massey, P., & Meynet, G. 2012, ApJ, 750, 97
Drout, M. R., Massey, P., Meynet, G., Tokarz, S., & Caldwell, N. 2009, ApJ, 703, 441
Fabrika, S., Sholukhova, O., Becker, T., et al. 2005, A&A, 437, 217
Glatzel, W. 2005, in ASP Conf. Ser. 332, The Fate of the Most Massive Stars, ed. R. M. Humphreys & K. Z. Stanek (San Francisco, CA: ASP), 22
Gordon, K. D., Clayton, G. C., Misselt, K. A., Landolt, A. U., & Wolff, M. J. 2003, ApJ, 594, 279
Gratier, P., Braine, J., Rodriguez-Fernandez, N. J., et al. 2010, A&A, 522A, 3
Groh, J. H., Hillier, D. J., Damineli, A., et al. 2009, ApJ, 698, 1698
Hubble, E. 1929, ApJ, 69, 103
Hubble, E., & Sandage, A. 1953, ApJ, 118, 353
Humphreys, R. M. 1975, ApJ, 200, 426
Humphreys, R. M. 1978, ApJ, 219, 445
Humphreys, R. M., & Davidson, K. 1994, PASP, 106, 1025
Humphreys, R. M., Davidson, K., Gordon, M. S., et al. 2014, ApJL, 782, L21
Humphreys, R. M., Davidson, K., Grammer, S., et al. 2013a, ApJ, 773, 46 (Paper I)
Humphreys, R. M., Davidson, K., & Smith, N. 1999, PASP, 111, 1124
Humphreys, R. M., Jones, T. J., & Gehrz, R. D. 1987, AJ, 94, 315
Humphreys, R. M., Jones, T. J., Polomski, E., et al. 2006, AJ, 131, 2105
Humphreys, R. M., Leitherer, C., Stahl, O., Wolf, B., & Zickgraf, F.-J. 1988, A&A, 203, 306
Humphreys, R. M., & Sandage, A. 1980, ApJS, 44, 319
Humphreys, R. M., Weis, K., Burggraf, B., et al. 2013b, ATel, 5362
Johansson, S. E., & Letokhov, V. S. 2004, A&A, 428, 497
Kaluzny, J., Stanek, K. Z., Krockenberger, M., et al. 1998, AJ, 115, 1016
Knapp, G. R., Kerr, F. J., & Rose, W. K. 1973, ApL, 14, 187
Kraus, M., Cidale, L. S., Arias, M. L., Oksala, M. E., & Borges Fernandes, M. 2014, ApJL, 780, L10
Leitherer, C., Allen, R., Altner, B., et al. 1994, ApJ, 428, 292
Luyten, W. J. 1928, BHarO, 859, 1
Martins, F., Schaerer, D., & Hillier, D. J. 2005, A&A, 436, 1049
Massey, P. 2006, ApJL, 638, L93
Massey, P., Bianchi, L., Hutchings, J. B., & Stecher, T. P. 1996, ApJ, 469, 629
Massey, P., Bresolin, F., Kudritzki, R. P., Puls, J., & Pauldrach, A. W. A. 2004, ApJ, 608, 1001
Massey, P., & Johnson, O. 1998, ApJ, 505, 793
Massey, P., McNeill, R. T., Olsen, K. A. G., et al. 2007, AJ, 134, 2474
Massey, P., Olsen, K. A. G., Hodge, P. W., et al. 2006, AJ, 131, 2478
McQuinn, K. B. W., Woodward, C. E., Willner, S. P., et al. 2007, ApJ, 664, 850
Mokiem, M. R., de Koter, A., Evans, C. J., et al. 2007, A&A, 465, 1003
Monteverde, M. L., Herrero, A., Lennon, D. J., et al. 1996, A&A, 312, 24
Mould, J., Barmby, P., Gordon, K., et al. 2008, ApJ, 687, 230
Oksala, M. E., Kraus, M., Cidale, L. S., Muratore, M. F., & Borges Fernandes, 2013, A&A, 558, A17
Owocki, S., & Shaviv, N. 2012, in Eta Carinae and the Supernova Impostors, Astrophysics & Space Science Library Vol. 384, ed. K. Davidson & R. M. Humphreys (New York: Springer), 275
Peeters, E., Tielens, A. G. G. M., Roelfsema, P. R., & Cox, P. 1999, in The Universe as Seen by ISO., ed. P. Cox & M. F. Kessler, ESA-SP 427, 739
Polcaro, V. F., Gualandi, R., Norci, L., Rossi, C., & Viotti, R. F. 2003, A&A, 411, 993
Polcaro, V. F., Rossi, C., Viotti, R. F., et al. 2011, AJ, 141, 18
Romano, G. 1978, A&A, 67, 291
Rosino, L., & Bianchini, A. 1973, A&A, 22, 453
Sandage, A., & Tammann, G. A. 1974, ApJ, 191, 603
Savage, B. D., & Jenkins, E. B. 1972, ApJ, 174, 491
Sharov, A. S. 1973, Perem. Zvezdy, Byull., Tom, 19, 3
Shemmer, O., Leibowitz, E. M., & Szkody, P. 2000, MNRAS, 311, 698
Sholukhova, O. N., Fabrika, S. N., Roth, M., & Becker, T. 2004, BaltA, 13, 156
Sholukhova, O. N., Fabrika, S. N., Zharova, A. V., Valeev, A. F., & Goranskij, V. P. 2011, AstBu, 66, 123
Smith, L. J., Crowther, P. A., & Prinja, R. K. 1994, A&A, 281, 833
Stahl, O., Jankovics, I., Kovács, J., et al. 2001, A&A, 375, 54
Szeifert, T., Humphreys, R. M., Davidson, K., et al. 1996, A&A, 314, 131
Thompson, T. A., Prieto, J. L., Stanek, K. Z., et al. 2009, ApJ, 705, 1364
Tielens, A. G. G. M., Hony, S., van Kerckhoven, C., & Peeters, E. 1999, in The Universe as Seen by ISO., ed. P. Cox & M. F. Kessler (ESA-SP 427; Noordwijk: ESA), 579
Valeev, A. F., Sholukhova, O. N., & Fabrika, S. N. 2010, AstBu, 65, 381
van den Bergh, S., Herbst, E., & Kowal, C. T. 1975, ApJS, 29, 303
Van Dyk, S. D. 2005, in ASP Conf. Ser. 332, The Fate of the Most Massive Stars, ed. R. M. Humphreys & K. Z. Stanek (San Francisco, CA: ASP), 47
Van Dyk, S. D., & Matheson, T. 2012, in Eta Carinae and the Supernova Imposters, Astrophysics & Space Science Library, Vol. 384, ed. K. Davidson & R. M. Humphreys (New York: Springer), 249
van Genderen, A. M., & Sterken, C. 2002, A&A, 386, 926
Vink, J. S. 2012, in Eta Carinae and the Supernova Imposters, Astrophysics & Space Science Library, Vol. 384, ed. K. Davidson & R. M. Humphreys (New York: Springer), 221
Viotti, R. F., Rossi, C., Polcaro, V. F., et al. 2006, A&A, 458, 225
Wolf, B. 1989, A&A, 217, 87
Wright, E. L., Eisenhardt, P. R. M., Mainzer, A. K., et al. 2010, AJ, 140, 1868